An Experimental Investigation into Diesel Engine Exhaust Waste Heat Recovery for Water Purification

A Dissertation submitted
in partial fulfillment of the requirements
for the degree of

Master of Engineering
in
Thermal Engineering

by
Arashdeep Singh
Registration No.: 801483027

Under the Supervision of
Mr. Sumeet Sharma
(Associate Professor)

MECHANICAL ENGINEERING DEPARTMENT
THAPAR UNIVERSITY, PATIALA, INDIA

July, 2016

CERTIFICATE

I hereby declare that the thesis entitled **"An Experimental Investigation into Diesel Engine Exhaust Waste Heat Recovery for Water Purification"** is an authentic record of my work carried out as requirements for the award of the degree of **Master of Engineering** in **Thermal Engineering** at **Thapar University, Patiala** under the supervision of **Mr. Sumeet Sharma,** Associate Professor, Mechanical Engineering Department, Thapar University, Patiala during July, 2014 to July, 2016. No part of this matter embodied in this report has been submitted to any other university or institute for the award of any degree.

Arashdeep Singh

Date: 11/07/2016
Place: Patiala, India

Arashdeep Singh
(801483027)

It is certified that the above statement made by the student is correct to the best of my knowledge and belief.

Sumeet Sharma

Mr. Sumeet Sharma
(Associate Professor)
Mechanical Engineering Department
Thapar University, Patiala – 147004, India

Countersigned by

Dr. S.K. Mohapatra
Senior Professor and Head
Mechanical Engineering Department
Thapar University, Patiala – 147004, India

Dr. S.S. Bhatia
Dean of Academic Affairs
Thapar University, Patiala – 147004, India

Dedicated to

my parents

S. Balwinder Singh & Smt. Surinder Paul Kaur

and

to my sister Navjot

This work is a sign of my love to you!

Acknowledgement

I would like to express my deepest gratitude to my supervisor, Mr. Sumeet Sharma, Associate Professor, Mechanical Engineering Department, Thapar University for his valuable guidance, motivation, patience and providing me with an excellent atmosphere for doing research. Your advice on both research as well as on my career have been priceless. It has been a great pleasure and experience to work under your sanctuary.

I am heartily thankful to Dr. S.K. Mohapatra, Senior Professor and Head, Mechanical Engineering Department for his continuous help. The opportunity, support, exposure and atmosphere provided by the Thapar University, Patiala, to carry out my studies are highly appreciated.

A special debt of gratitude is owed to the authors whose works I have consulted and quoted in this work. Last but not the least, I am forever grateful to my parents, family and friends for their love, encouragement, unconditional support and best wishes.

Arashdeep Singh

Arashdeep Singh

Abstract

About 30% of the total combustion heat of an IC engine is carried away by the outgoing exhaust flue gases. This exhaust waste heat can be used for the purification of water. In the present work, a waste heat recovery cum water purification unit consisting of horizontal tube submerged evaporator and water cooled condenser was designed, fabricated and integrated to a 3.5 kW variable compression ratio diesel engine to perform purification of ground water. For this analysis, four hand pump water samples were collected from different areas of the '*Malwa'* region of Indian Punjab *viz.* Kotkapura, Faridkot, Sri Muktsar Sahib and Bathinda. The collected water samples were tested for physico-chemical parameters and presence of heavy metals before and after performing distillation. The TDS content and level of some of the heavy metals like Zn, Pb and Fe were found to be quite high in the collected water samples. The experiments for distilled water collection rate were performed at four different compression ratios *viz.* 12:1, 14:1, 16:1 and 18:1 and at five loading conditions *i.e.* 2 kg, 4 kg, 6 kg, 8 kg and 10 kg. The distilled water collection rate was found to be directly proportional to the amount of recoverable heat from the diesel engine. The maximum and minimum collection rate observed were 2.75 LPH and 0.22 LPH noted respectively at CR – 12:1 / 10 kg load and CR – 18:1 / 2 kg load. The level of physico-chemical parameters and heavy metals in the resulting distilled water was found to be well below the limits defined by WHO and BIS. In this work, a comparison between collected distilled and RO water with respect to purity level is also presented. At the end, a discussion into total cost and payback period of the proposed unit is made. The payback period for the normal working of 8 hours per day, at maximum collection rate was found to be 2 years. This proposed water purification unit can be integrated with stationary IC engines, ships etc. for water purification / desalination purpose, thus, can impact a large population of the world.

***Keywords*:** Diesel engine exhaust; Waste heat recovery; Heat exchanger; Physico-chemical parameters; Heavy metals; Water purification.

Table of Contents

List of Figures

List of Tables

Nomenclature

A_{hc}	=	Condenser heat transfer area, m^2
A_{he}	=	Evaporator heat transfer area, m^2
A_s	=	Heat transfer surface area, m^2
C_f	=	Correction factor
C_c	=	Correction factor for condenser
C_e	=	Specific heat capacity of exhaust gas, kJ/kgK
C_d	=	Specific heat capacity of distillate water, kJ/kgK
C_{gw}	=	Specific heat capacity of ground water, kJ/kgK
d_{ci}	=	Internal diameter of the condenser tubes, m
d_{co}	=	External diameter of the condenser tubes, m
d_{csi}	=	Internal diameter of the condenser shell, m
d_{ei}	=	Internal diameter of the evaporator tubes, m
d_{eo}	=	External diameter of the evaporator tubes, m
d_{esi}	=	Internal diameter of the evaporator shell, m
d_i	=	Internal diameter of the tube, m
d_o	=	External diameter of the tube, m
FR_{ci}	=	Fouling resistance at the inside of condenser, m^2K/W
FR_{co}	=	Fouling resistance at the outside of condenser, m^2K/W
FR_{ei}	=	Fouling resistance at the inside of evaporator, m^2K/W
FR_{eo}	=	Fouling resistance at the outside of evaporator, m^2K/W
FR_i	=	Inside fouling resistance, m^2K/W
FR_o	=	Outside fouling resistance, m^2K/W
h_{ci}	=	Condenser inside heat transfer coefficient, W/m^2K
h_{co}	=	Condenser outside heat transfer coefficient, W/m^2K
h_{ei}	=	Evaporator inside heat transfer coefficient, W/m^2K
h_{eo}	=	Evaporator outside heat transfer coefficient, W/m^2K
h_f	=	Specific enthalpy of saturated liquid, kJ/kg
h_{fg}	=	Latent heat, kJ/kg

h_i = Inside heat transfer coefficient, W/m^2K

h_o = Outside heat transfer coefficient, W/m^2K

K_e = Thermal conductivity of exhaust gas, W/mK

K_{gw} = Thermal conductivity of ground water, W/mK

K' = Thermal conductivity of copper, W/mK

K_t = Thermal conductivity of tube material, W/mK

l_c = Total length of the condenser copper tube, m

l_{cs} = Length of the condenser shell, m

l_e = Length of the evaporator copper tube, m

l_{es} = Length of the evaporator shell, m

L_{gw} = Latent heat of vaporization of ground water, kJ/kg

L_{st} = Latent heat of steam, kJ/kg

$\dot{m}_{dw}$ = Distilled water mass flow rate, kg/s

$\dot{m}_e$ = Exhaust gas mass flow rate, kg/s

$\dot{m}_{gw}$ = Ground water mass flow rate, kg/s

$\dot{m}_{st}$ = Steam mass flow rate, kg/s

N_c = Total number of copper tubes in the condenser

N_e = Total number of copper tubes in the evaporator

Nu_c = Nusselt number for condenser

Nu_e = Nusselt number for evaporator

P = Temperature effectiveness, defined by Eq. (4.18)

Pr_c = Prandtl number for condenser

Pr_e = Prandtl number for evaporator

Q = Total rate of heat transfer, kW

Q_c = Heat load on the condenser, kW

Q_e = Amount of actual extractable heat from exhaust flue gas, kW

Q_{max} = Maximum amount of recoverable heat from exhaust flue gas, kW

Q_r = Amount of energy required for water evaporation, kW

R = Heat capacity rate ratio, defined by Eq. (4.17)

Re_c = Reynolds number for condenser

Re_e = Reynolds number for evaporator

T_{bw} = Boiling point temperature of water, K

T_{c1} = Cold fluid temperature at the inlet, K

T_{c2} = Cold fluid temperature at the outlet, K

T_{dwi} = Distilled water temperature at condenser inlet, K

T_{dwo} = Distilled water temperature at condenser outlet, K

T_{ei} = Exhaust gas temperature at evaporator inlet, K

T_{eo} = Exhaust gas temperature at evaporator outlet, K

T_g = Flue gas temperature, K

T_{gwi} = Ground water temperature at condenser inlet, K

T_{gwo} = Ground water temperature at condenser outlet, K

T_{h1} = Hot fluid temperature at the inlet, K

T_{h2} = Hot fluid temperature at the outlet, K

ΔT_{dw} = Variation in temperature of distillate water, K

ΔT_{gw} = Variation in temperature of ground water, K

ΔT_i = Variation in local temperature of two fluids at the inlet, K

ΔT_{lmc} = Logarithmic mean temperature difference for condenser, K

ΔT_{lme} = Logarithmic mean temperature difference for evaporator, K

ΔT_m = Logarithmic mean temperature difference, K

ΔT_o = Variation in local temperature of two fluids at the outlet, K

U = Overall heat transfer coefficient, K

U_{oc} = Overall heat transfer coefficient of double pass condenser, W/m^2K

U_{oe} = Overall heat transfer coefficient of single pass evaporator, W/m^2K

V_c = Velocity of the ground water through the condenser tube, m/s

V_e = Velocity of the exhaust flue gas passing through the evaporator tubes, m/s

V_{sw} = Swept volume of the engine, m^3

V_{cl} = Clearance volume of the engine, m^3

Greek Symbols

Δ = Variation or difference

μ_c = Dynamic viscosity of the ground water, Pa.s

μ_e = Dynamic viscosity of the exhaust gas, Pa.s

ρ_c = Density of the ground water, kg/m^3

ρ_e = Density of the exhaust flue gas, kg/m^3

Φ = Function of

Chemical Symbols

Al = Aluminum

As = Arsenic

Ca = Calcium

Cd = Cadmium

Co = Cobalt

CO = Carbon monoxide

CO_x = Carbon oxides

Cr = Chromium

F- = Fluoride

Fe = Iron

HC = Hydrocarbons

K = Potassium

Mg = Magnesium

Na = Sodium

NaCl = Sodium chloride

Ni = Nickel

NO_x = Nitrogen oxides

Pb = Lead

Se = Selenium

SO_2 = Sulpher dioxide

Zn = Zinc

Acronyms

AERB	≡	Atomic Energy Regulatory Board
AES	≡	Atomic emission spectroscopy
BIS	≡	Bureau of Indian Standards
CI	≡	Compression ignition
CR	≡	Compression ratio
IC	≡	Internal combustion
LMTD	≡	Logarithmic mean temperature difference
LPH	≡	Liters per hour
MP-AES	≡	Microwave plasma atomic emission spectrometer
ppm	≡	Parts per million
RO	≡	Reverse osmosis
SI	≡	Spark ignition
TEMA	≡	Tubular Exchanger Manufacturers Association
TDS	≡	Total dissolved solids
VCRE	≡	Variable compression ratio engine
WHO	≡	World Health Organization

Chapter 1

Introduction

Energy is an important entity responsible for economic growth, urbanization, industrialization and improvement of quality of life in the society. Abrupt rise in energy demand due to growing population and industrialization, depleting fossil fuel resources and compilation with international protocols on environment and climatic change has pushed the world to think about alternative sources of energy and methodologies for energy conservation [Pandiyarajan et al., 2011]. Today, World relies heavily on IC engines for transportation, power generation and pumping of water. The CI or diesel engines are having wide range of applications in day to day life due to their reliability and easy starting [Maheswari et al., 2015]. Although many improvements have been made to increase the efficiency of diesel engines yet a considerable quantity of heat energy is rejected to the surroundings through outgoing exhaust flue gases, coolant and lubricating oil, and friction. This heat dumped into the surroundings which otherwise can be used for some economic or useful purposes is called waste heat [Bari and Hossain, 2013; Pandiyarajan et al., 2011]. The utilization of the exhaust waste heat of an IC engine has many advantages like it increases thermal efficiency of the engine, decreases fuel consumption, emissions and size of the components. Additionally, the thermal pollution and noise level also decreases [Jadhao and Thombare, 2013].

The exhaust flue gas has large recovery potential due to its high exergy and temperature [He et al., 2011]. Many new technologies/methods like thermoelectric energy conversion, turbocharging and Rankine bottoming cycle working on the basis of waste heat recovery have been developed by various researchers [Saidur et al., 2012]. The exhaust waste heat can be stored in a thermal storage medium by employing sensible and latent heat storage mediums using finned shell and tube heat exchanger [Pandiyarajan et al., 2011]. It has been noted that the recovery of the exhaust waste heat results in additional power generation. An additional power generation of 23.7% was noted after optimization of the heat exchanging unit [Bari and Hossain, 2013]. The recoverable heat from an IC engine can be increased by using a combined thermodynamic cycle consisting both organic Rankine cycle and Kalina cycle [He et al., 2011]. A reduction in NO_x, CO_x and particulate emission and an increase in the overall efficiency of the

engine were observed with utilization of the exhaust waste heat of an IC engine [Lee et al., 2010].

Waste heat can also be employed for the purification of water. Potable water is absolutely necessary for the development of human body. Moreover, economic growth of any nation depends heavily on the availability of water resources. Out of the total water available on Earth, only 3% is considered fit for drinking purpose. It has been noted that approximately 25% of the total population of the World does not have access to safe drinking water [Karagiannis and Soldatos, 2008]. Moreover, due to anomalous weather conditions caused by global warming, poor waste and sewage water management, plus water pollution caused by agricultural and industrial wastes, more than 65% of the population of the World may experience the water shortage by 2025 [Tanaka and Park, 2010; Karagiannis and Soldatos, 2008].

Many studies have been conducted by various researchers to utilize waste heat for water purification. Maheswari et al. [2015] utilized the exhaust waste heat of an IC engine having rated power 5 HP for desalination of saline water. Fresh water collection rate per hour with preheating at maximum load was found to be 3 liters. Tanaka and Park [2010] employed the waste heat from a portable electric generator as a heat source for increasing the productivity of desalinated water in solar stills. Approximately 20 liters of distilled water can be produced with an operational time of about 9 hours. Additionally, in an another study, the waste heat from thermal power plant was utilized for the optimization of water production and performance ratio of multi stage flash distillation and multi effect distillation plants [Sommariva, 2008]. Moore et al. [2008] designed a new sub-atmospheric pressure based water distillation system. This system requires low temperature to boil water and can run by using low quality heat energy sources like waste heat of an IC engine. Cardona et al. [2007] recovered the waste heat from the cooling system and exhaust flue gases of a reciprocating natural gas engine and fed it to a small desalination system for purification of water. The advantages with this coupled unit were reduced fresh water cost, less thermal pollution and significant power savings. Rahman et al. [2003] utilized waste heat of an engine to produce both power and water using submerged vertical tube evaporator. Kalogirou [2001] designed a low cost spray type evaporator in which saline water was sprayed into fine droplets for evaporation resulting in desalination of seawater. The annual production with 1 m^2 of solar collector area was about 11.2 m^3. Therefore, many waste heat recovery systems have been designed in the past.

The need for fresh water in India is growing day by day due to poor quality of water, population explosion, industrial growth and ground water pollution. The drinking water quality issues are very serious in the '*Malwa'* belt of Indian Punjab. The large use of pesticides and fertilizers for the agricultural growth, poor human activities, chemical waste of industries, poor solid waste management and fly ash from thermal power plants has resulted into poor quality of groundwater [Bajwa et al., 2015; Sekhon and Singh, 2013; Tripathi et al., 2013; Singh, 2008; Mehra et al., 2007]. The content of uranium present in the drinking water samples of four districts of Punjab was investigated. Out of the total 498 samples analyzed, 68% surpass the safe limit defined by WHO and 43% exceed the safe limit given by AERB. Also, the concentration of heavy metals like As, Pb, Ni, Zn and Cr and physico-chemical parameter – TDS was found to be above the safe limits defined by WHO [Bajwa et al., 2015]. The average value of uranium concentration in Punjab was found to be 72.9 µg/l, which was above the guideline values defined at national and international level [Tripathi et al., 2013]. In addition to this, the investigation was carried out for the presence of heavy metals in the water samples collected from tube wells of 100 different locations of the Patiala district of Punjab, India. After analysis, using atomic absorption spectroscopy technique, high level of nickel and aluminum were observed in most of the water samples [Sekhon and Singh, 2013]. Therefore, the quality of water in the *'Malwa'* region of Indian Punjab is very poor. The presence of physico-chemical parameters and heavy metals in high concentration in the drinking water has many adverse effects on the human body. It can cause cancer, diarrhea, genetic disorders obstruct mental development and damage blood vessels [W.1].

The aim of most of the existing waste heat recovery systems is to perform desalination of saline water. Very limited work has been done to remove heavy metals and other physico-chemical compounds from the drinking water. Thus, further research is needed to be carried out to curb this issue of poor water quality. Large numbers of diesel and stationary engines are used for the agriculture purpose in Punjab. The exhaust waste heat of these engines can be a potential source for the distillation of water. The aim of this thesis work is to utilize exhaust waste heat of an IC engine for performing distillation of ground water. For this purpose, a portable heat exchanging unit is needed to be designed which can easily be integrated with an IC engine to perform distillation.

Chapter 2

Literature review

This chapter presents the studies and research carried out by different researchers in the vicinity of waste heat recovery and water purification. In the initial part of this chapter, a discussion into waste heat recovery, water scarcity, heat exchangers, LMTD and fouling has been made. In the later section, various techniques developed for water purification along with some specific investigations conducted by different researchers are presented.

2.1. Waste heat and its utilization

Energy is responsible for holistic development of any nation. In socio-economic outlook, the consumption of energy in a particular country is directly proportional to the total population and economic growth. Due to increasing population and fast development of the urban areas, the transportation sector is put under an essential role [Saidur et al., 2012]. It has been noted that about 29.5% of the total energy consumption in the World is consumed by the transportation sector alone [Jia et al., 2009].

Today, CI and SI engines are mostly used to power vehicles. Due to higher efficiency of CI or diesel engines, they are having a wide range of applications. Regardless of the developments in the area of IC engines, a large amount of chemical energy of the fuel in the form of heat energy goes waste to the surroundings through coolant, lubricating oil, exhaust flue gas and friction. Therefore, only a small portion of energy is obtained as a useful shaft work. Waste heat is generally the heat which is generated in a process by means of chemical reaction or combustion of fuel, and then discarded into the surroundings. This dumped heat can be used for some other applications thus giving economic advantages.

It has been found that at full loading conditions, a diesel engine can only convert approximately 38% of the total available energy into useful crankshaft work [Taymaz, 2006]. The temperature inside an IC engine is very high which can never be with stand by the engine materials. So, to exchange heat from the engine, cooling system is provided in which a coolant takes up the heat from the engine and maintain proper temperature. As shown in Fig. 2.1, about 25% of the total available energy goes waste through the cooling and lubrication system, 30%

through outgoing exhaust flue gas and 7% through frictional losses [Yu and Chau, 2009]. Thus, a large amount of heat goes waste in the form of exhaust flue gas which can be recovered for other applications due to its high exergy potential and temperature.

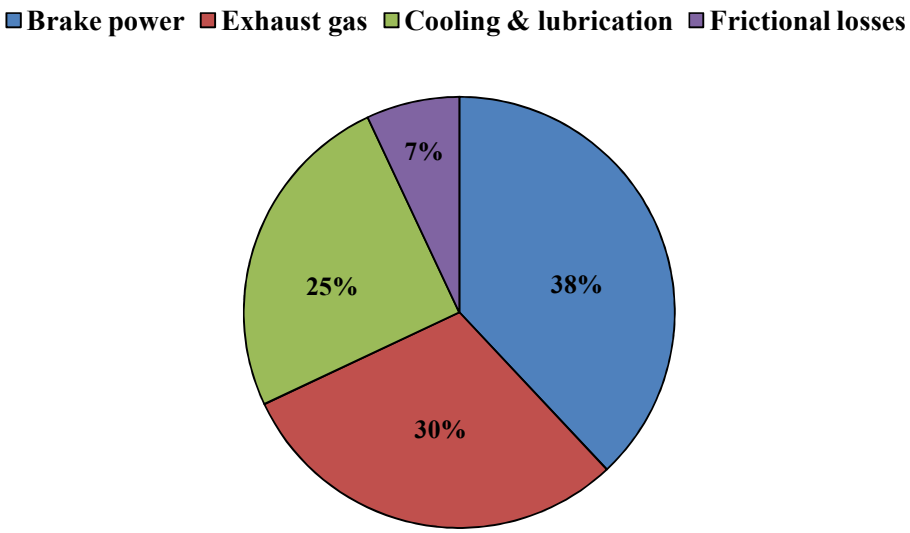

Figure 2.1: Total content of the fuel energy in a diesel engine [Yu and Chau, 2009]

Some of the technologies developed for utilization of the waste heat from IC engines are given below:

i. Thermoelectric energy conversion

Thermoelectric generators (TEG) are one of the new capable devices for waste heat recovery of IC engines. Using these generators, the thermal energy available in the engine exhaust is converted into electrical energy on the basis of Seebeck effect. For this conversion, heat exchanger, power conditioning system, TEG system and battery pack are used. The thermal energy of the exhaust flue gas is stored in the heat exchanger placed next to the catalytic converter. This stored power is transferred to the TEG system where electricity is generated [Saidur et al., 2012]. The complete thermoelectric energy conversion system is illustrated in Fig. 2.2. These conversion systems are having silent operation, free maintenance and high reliability. In addition to this, using these systems, an increase in engine performance and fuel efficiency is usually observed.

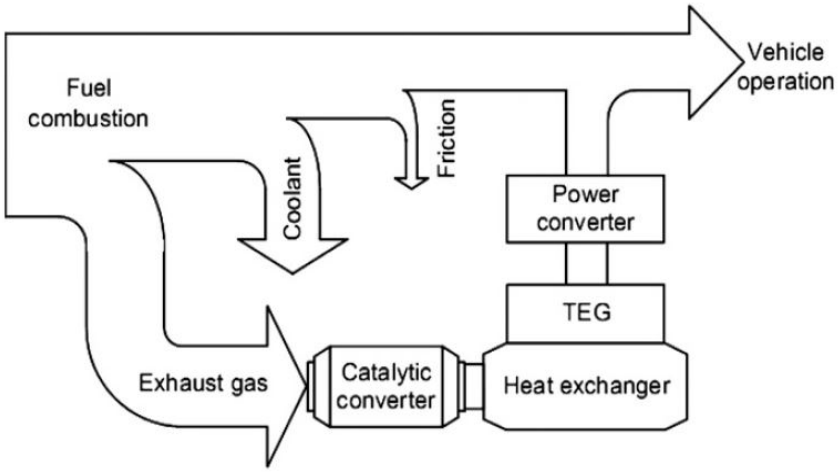

Figure 2.2: Thermoelectric energy conversion based waste heat recovery system [Yu and Chau, 2009]

ii. Turbocharging

The outgoing exhaust flue gas of an IC engine has high temperature and pressure which can be used to increase the power of the engine with compression of the air going into the combustion chamber. For this purpose, turbocharger is used. Turbocharger is basically a gas turbine consisting of actuator, waste gate valve, compressor, shaft and turbine. A turbocharger is shown in Fig. 2.3. With turbocharging, engine size and particulate emission decreases. Turbocharging also increases the fuel economy of the engine by 30% – 50% [Saidur et al., 2012]. The only difference between the turbocharger and supercharger is that turbocharger is driven by the exhaust energy whereas the supercharger is run by the shaft power using a belt drive.

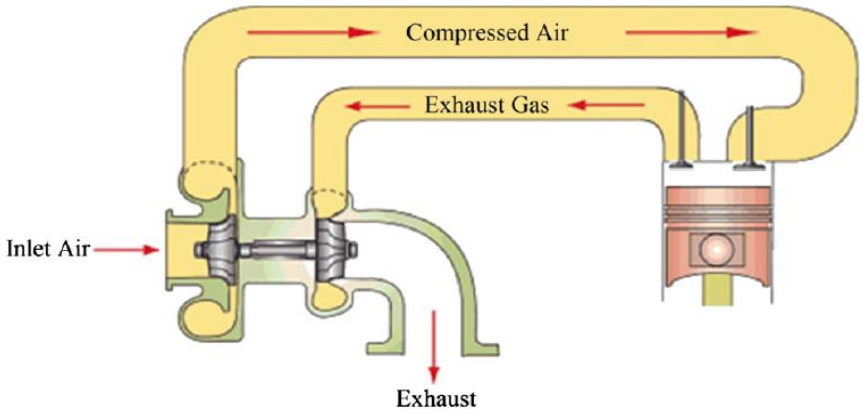

Figure 2.3: Waste heat recovery using turbocharger [Pickerill, 2010]

iii. Rankine bottoming cycle

The layout of the Rankine bottoming cycle is depicted in Fig. 2.4. This cycle is a derivative of the Rankine cycle and consists of an evaporator/boiler, expander, condenser and a pump. The efficiency of the cycle varies with the system operating conditions and the kind of working fluid used. The evaporator takes up the heat from the exhaust flue gas and steam so formed is further got expanded using an expansion device called expander. The heat energy of the fluid is released using a condenser and fluid comes in the liquid state. Finally, it is pumped to the boiler starting the whole cycle again [Hasanuzzaman et al., 2011; Vaja and Gambarotta, 2010]. A 10% decrease in fuel consumption of the passenger cars is noted using Rankine bottoming cycle [Hountalas et al., 2012; Ibaraki et al., 2007].

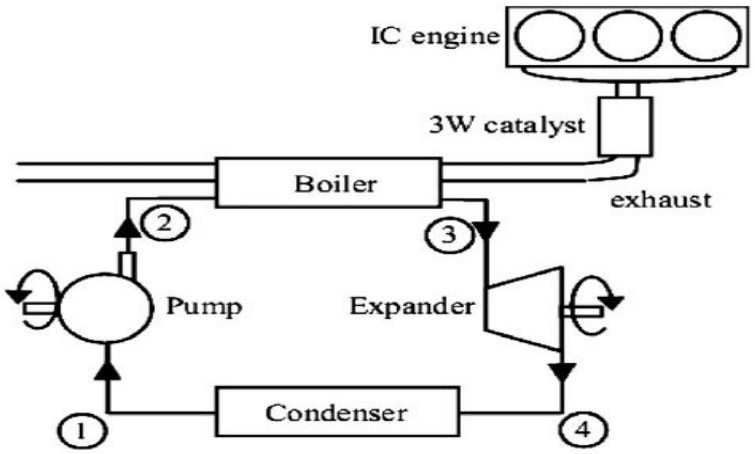

Figure 2.4: Waste heat recovery using Rankine bottoming cycle [Duparchy et al., 2009]

2.2. Advantages of waste heat recovery

Waste exhaust heat from diesel engines can be recovered for different purposes like thermoelectric generation, Rankine bottoming cycle, desalination/water purification and turbocharging. The waste heat recovery from IC engines has many advantages which are listed below [Jadhao and Thombare, 2013]:

i. Combustion process efficiency of the engine becomes better which reduces the total process cost.
ii. The thermal efficiency of the engine increases.

iii. The fuel consumption of the engine decreases because more dense pressurized air is going into the combustion chamber due to turbocharging.

iv. Due to reduction in the fuel consumption of the engine, the quantity of the exhaust flue gas falls down which decreases the size of the equipments.

v. The decrease in the size of various equipments reduces the auxiliary energy consumption by various components like fans, pumps, etc.

vi. Due to better mixing of preheated air with the diesel fuel in the combustion chamber, the CO emissions from the engine decreases.

vii. Turbocharging increases the inlet temperature of the air going into the system due to which the ignition delay gets reduced resulting in lower NO_x emission.

viii. The exhaust gas temperature after the heat recovery is less which decreases the thermal pollution and helps to reduce global warming.

ix. Due to better combustion and uniform fuel mixing, the engine noise level decreases.

2.3. Water scarcity

Water is vital for all human beings. It covers 71% of the Earth's surface. Nearly 96% of the water on Earth is found in seas and oceans which are not considered safe for drinking purpose due to the presence of high salt content in it. Remaining 1.7% is found in groundwater, 2% in glaciers of Greenland and Antarctica, and a little part is found in other large water bodies. Just 2.5% of Earth's water is considered as fresh water, out of which 98.8% is present in the form of groundwater and ice. Other 0.3% of water is found in lakes and rivers [W.16].

Safe drinking water is essential for human beings but approximately 1.2 billon people are still lacking access to safe drinking water [W.19]. This lack of sufficient water availability in a particular region has led to the impasse of water scarcity. The reasons for water scarcity are many like inefficient use of water for irrigation and domestic purposes, poor wastewater and sewage management, release of effluents and chemicals to the rivers, industrialization, urbanization and environmental pollution.

The problem of water scarcity due to poor water quality and water pollution exists in India too. More specifically, according to recent reports, in the *'Malwa'* belt of Indian Punjab, the groundwater contains uranium and heavy metals in an amount more than the maximum prescribed limit defined by WHO and AERB [Bajwa et al., 2015; Sekhon and Singh, 2013;

Tripathi et al., 2013; Singh, 2008; Mehra et al., 2007]. Out of total 498 drinking water samples analyzed by the researchers, 68% surpass the safe limit given by WHO and 43% exceed the safe limit defined by AERB. Also, it has been noted that the content of heavy metals *viz.* As, Pb, Ni, Zn and Cr is above the safe limits given by WHO. These high concentrations might be due to natural geology, urbanization, release of industrial pollutants and large use of pesticides and fertilizers in this region [Bajwa et al., 2015]. One more study also confirmed that the use of pesticides and fertilizers is highest in Punjab and agricultural fires during the wheat season carries pesticides away with it and harm water bodies across the *'Malwa'* region [Singh, 2008].

Therefore, different methods are needed to be developed, to make the ground water fit for drinking purpose. Today, different techniques are available for the purification of water. Some of the techniques used widely in the world are listed in the following section.

2.4. Techniques for water purification

For purification of water, different techniques have been developed. Some of the techniques which are in mature stage and used throughout the World are written below:

i. *Filtration:* This technique is used to remove suspended particles present in water. The separation is generally performed by using rapid or slow sand filters. Nowadays, membrane filtration technique is also widely used. Using membrane filtration, suspended particles having size greater than 0.2 μm can be removed. The filtration technique has a large use in industry. However, the filtration technique is not able to remove substances that are dissolved in water like heavy metals, uranium, nitrates and phosphorous [W.17].

ii. *Reverse Osmosis (RO):* In this technique, pure water is obtained by passing pre-filtered water through a semi-permeable membrane using mechanical pressure. The applied mechanical pressure should be such that it should overcome the osmotic pressure. This technique is used to remove suspended particles, molecules, bacteria and ions from impure water. RO is one of the widely used water purification techniques due to its portable nature and simple operation. However, the membrane should be well maintained, otherwise, it can be colonized by algae and other life forms [W.12].

iii. *Ion exchange:* This technique is used for decontamination, separation and purification of water using ion exchange resins like zeolites and clay. The unwanted ions are replaced by resin ions. Two types of ion exchanger's *viz.* cation exchangers and anion exchangers are used for the exchanging purpose. This technique is widely used in chemical and petrochemical, power, semiconductor, metal finishing and pharmaceutical industries [W.9]. This technique is not able to remove uncharged organic molecules like viruses and bacteria.

2.5. Distillation and its types

The other water purification technique widely adopted is distillation. In this technique, selective evaporation and condensation is performed for the separation of different components from liquid substance. Through distillation, water of highest quality which is free from all contaminants can be obtained. The water obtained through distillation is mild acidic (pH < 6). Hence, pH neutralization is needed to be done using basic substances like calcium carbonate or magnesium oxide. Figure 2.5 shows distillation test setup for laboratory applications.

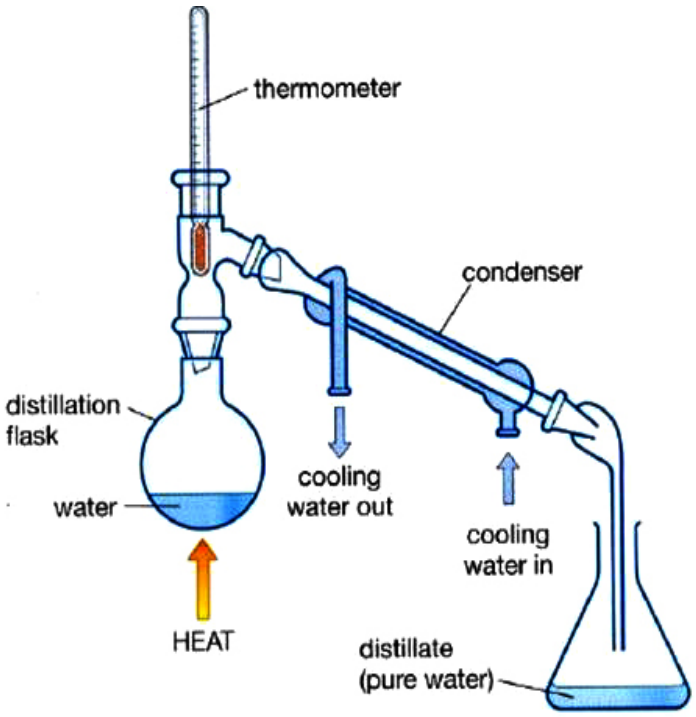

Figure 2.5: Distillation test setup for laboratory applications [W.5]

Distillation is used for the production of distilled beverages, crude liquid separation and air separation. The different type of distillation techniques are given below:

i. *Fractional distillation:* This type of distillation is used when the boiling points of different compounds present in a mixture are sufficiently close to each other. Repeated evaporation and condensation are performed in a fractionating packed column to perform distillation. This technique is mainly employed in the petroleum industry as it is used for the production of different petroleum components [W.4].

ii. *Steam distillation:* This technique is meant for the distillation of heat sensitive compounds. The raw material mixture is heated and steam is bubbled through it. According to the partial pressure, the targeted compound will vaporize. The vaporized mixture can then be condensed for separation [W.4].

iii. *Vacuum distillation:* Some compounds are having very high boiling points and these compounds cannot be evaporated easily. For such compounds, vacuum distillation technique is used. In this technique, the boiling pressure of the compounds is lowered. Once the pressure reaches the vapour pressure value at a particular given temperature, the evaporation commences and the rest of the distillation can be performed easily. This type of distillation is having large laboratory applications [W.4].

iv. *Molecular distillation:* It is a kind of vacuum distillation performed at a pressure of 0.01 torr. At this pressure, the fluids are in free molecular flow regime which means the size of the equipment is comparable to the mean free path of molecules. In this technique, the evaporation rate does not depend upon pressure as no significant pressure is exerted by the gaseous phase on the substance to be evaporated. This technique is used in industries for purification of oils [W.4].

v. *Membrane distillation:* In this technique, the partial vapor pressure difference is used for the separation process. This pressure difference is triggered by the temperature difference. Due to phase change, separation is enabled. The process uses a special hydrophobic membrane that acts as a barricade for the liquid phase but allows the water

vapors to lead through. This technique is generally used for seawater and brackish water desalination [W.4].

2.6. Heat Exchangers

Heat exchanger is a steady flow, open colossal system in which two flowing fluids exchange heat between themselves without losing or gaining any heat from the ambient. It works on the basis of second law of Thermodynamics *i.e.* heat is always transferred from higher temperature to lower temperature. The flowing fluids in the heat exchanger can have single phase or two phases. The mediums may or may not be in direct contact with each other. The transfer of heat in the heat exchanger takes place through conduction between the separating walls and convection in each fluid stream. The heat transfer rate between two fluid streams at a particular location depends upon the temperature difference at that location. Heat exchangers are having wide applications in industrial and domestic thermal systems. Prominent applications are in automobiles, thermal power plants, refrigeration and air-conditioning, chemical industries, petroleum refineries, heat recovery systems and alcohol industries.

2.6.1. Classification of heat exchangers

Different types of heat exchanger configurations are required for different heat transfer applications. Depending upon the requirements of heat transfer and other specified constraints, heat exchangers can be designed. Heat exchangers can be classified on the basis of flow arrangement, contact type, surface compactness and type of construction.

i. *Flow arrangement basis:* Heat exchangers may be of three types depending upon the kind of flow.

a. Parallel flow: When the direction of two fluid streams inside a heat exchanger is same than the flow is called parallel flow. The very unique character of this flow type is that temperature of hot fluid at exit will always be more than that of cold fluid at exit. Variation of temperature along the length of the heat exchanger is more pronounced in these heat exchangers so they are thermodynamically more irreversible. Figure 2.6 shows parallel flow regime in a double tube heat exchanger and Fig. 2.7 illustrates the associated temperature profile.

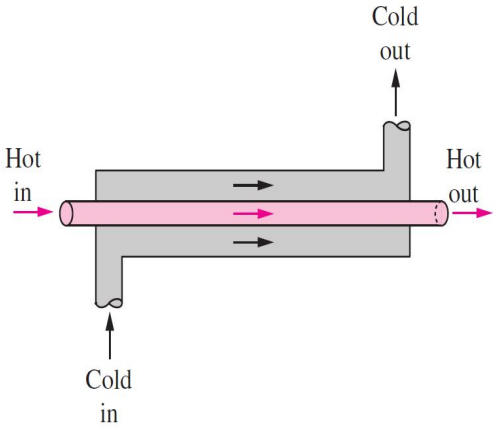

Figure 2.6: Parallel fluid flow in a double tube heat exchanger [Cengel, 2007]

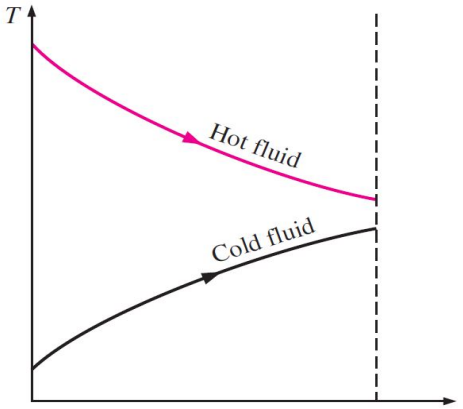

Figure 2.7: Temperature profile for parallel fluid flow [Cengel, 2007]

b. Counter flow: In this flow type, the fluid streams flow opposite to each other providing high heat exchange in less area. This type of flow has large applications due to its high LMTD and reversible nature. Counter flow regime in a double tube heat exchanger is shown in Fig. 2.8. Figure 2.9 depicts the corresponding temperature profile.

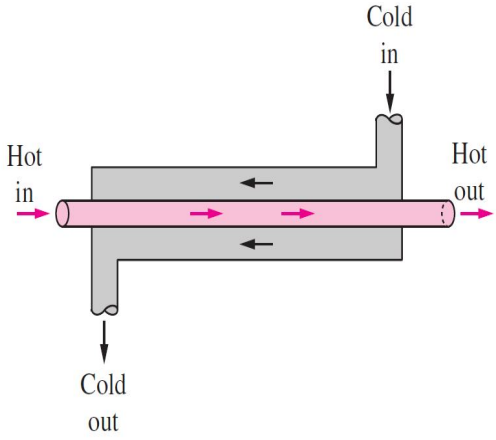

Figure 2.8: Counter fluid flow in a double tube heat exchanger [Cengel, 2007]

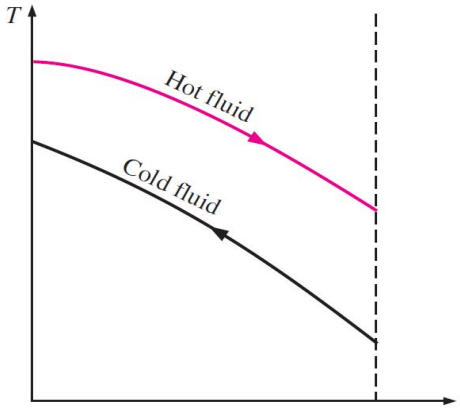

Figure 2.9: Temperature profile for for counter fluid flow [Cengel, 2007]

c. Cross flow: This is more of hybrid type in which flow patterns are not defined. Fluid streams cross each other at various points. This may further be divided into mixed or unmixed flow type. Mixed cross flow regime heat exchanger is illustrated in Fig. 2.10. Figure 2.11 depicts unmixed cross flow regime heat exchanger.

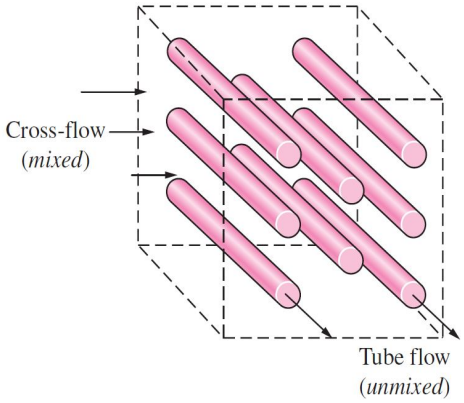

Figure 2.10: Mixed cross fluid flow [Cengel, 2007]

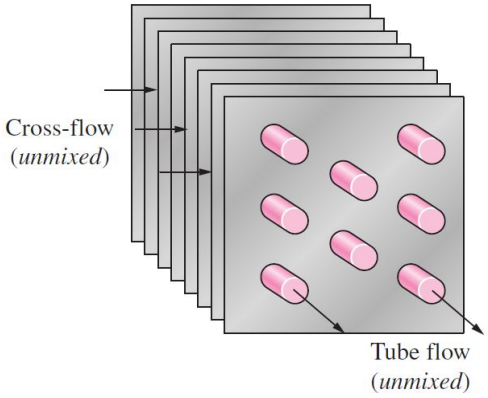

Figure 2.11: Unmixed cross fluid flow [Cengel, 2007]

ii. *Contact type basis:* Heat exchangers are of two types on the basis of contact between the fluid streams:

a. Direct contact type: Heat exchangers in which both hot and cold fluids gets physically mixed with each other while exchanging heat are called direct contact type heat exchangers. Jet condenser is an example of direct type heat exchangers.

b. Indirect contact type: The heat transfer between hot and cold fluids in indirect type heat exchangers occur through the wall of separation and not by physical mixing. Shell and tube type heat exchangers fall in this category.

iii. *Surface compactness basis:* On the basis of surface compactness, heat exchangers are classified into the following two types:

a. Compact heat exchangers: In this type, the ratio of the heat transfer surface area of a heat exchanger to its volume called the area density is greater than 700 m^2/m^3. High heat transfer rates in a small volume can be achieved through these heat exchangers. These heat exchangers are normally employed in applications with stringent restrictions on the weight and volume like radiators of automobiles.

b. Incompact type heat exchangers: In this type, the area density is lesser than 700 m^2/m^3.

iv. *On the basis of construction:* Heat exchanger on the basis of construction can be classified into three types *i.e.* tubular, extended surface type and plate type.

a. Tubular heat exchangers: These are shell and tube, spiral tube, and double pipe heat exchangers. Heat transfer takes place as one fluid flows outside the tubes through the shell while the other fluid flows inside the tubes. Figure 2.12 depicts shell and tube heat exchanger. The reasons for large usage of shell and tube heat exchangers are its easy adaptability to operating conditions, robustness, compactness and easy manufacturing.

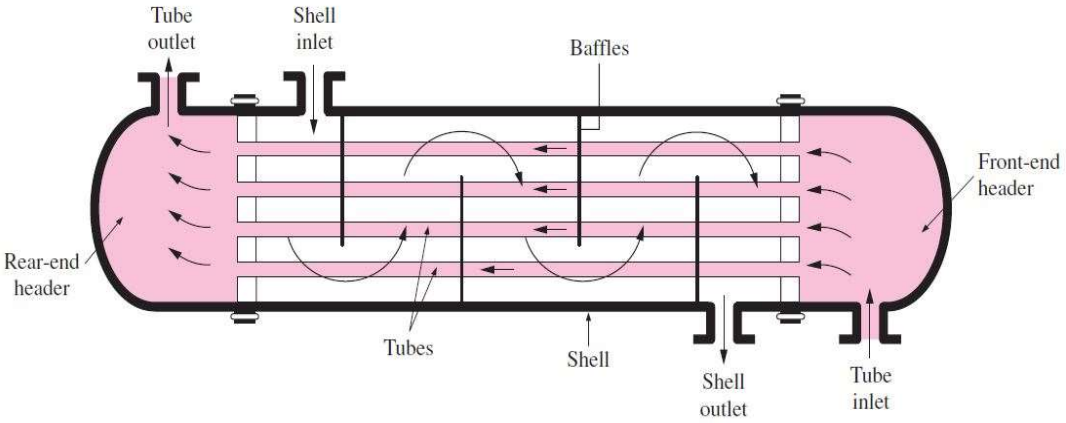

Figure 2.12: Shell and tube heat exchanger [Cengel, 2007]

b. Extended surface type heat exchangers: In this type of heat exchangers 'sandwiched' passages containing fins are used to increase the usefulness of the division. The designs include counter flow and cross flow attached with various fin configurations such as offset fins, straight fins and wavy fins. Figure 2.13 and Fig. 2.14 respectively shows finned tube and plate fin type heat exchanger (HE).

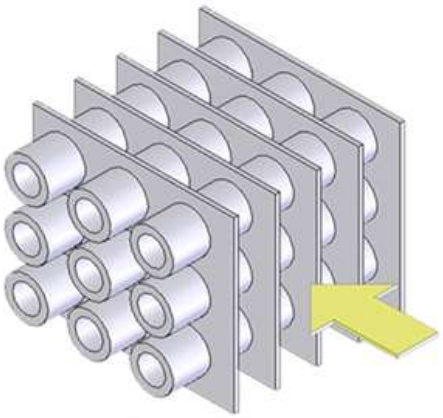

Figure 2.13: Finned tube HE [W.2]

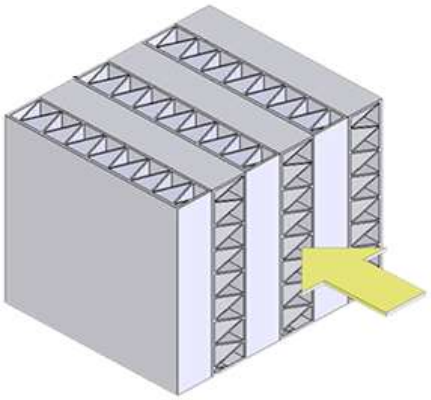

Figure 2.14: Plate fin HE [W.2]

c. Plate type heat exchangers: These heat exchangers can further be classified into plate and frame, spiral plate and pillow plate type. It consists of a number of plates in series with corrugated flat flow passages. The heat transfer in these configurations is often very efficient as cold and hot fluids flow in alternate passages and each cold fluid stream is surrounded by two hot fluid streams. More plates can be mounted if the demand for heat transfer increases. Figure 2.15 depicts plate type heat exchanger. Spiral plate heat exchanger is shown in Fig. 2.16. A complete classification of different type of heat exchangers is illustrated in Fig. 2.17.

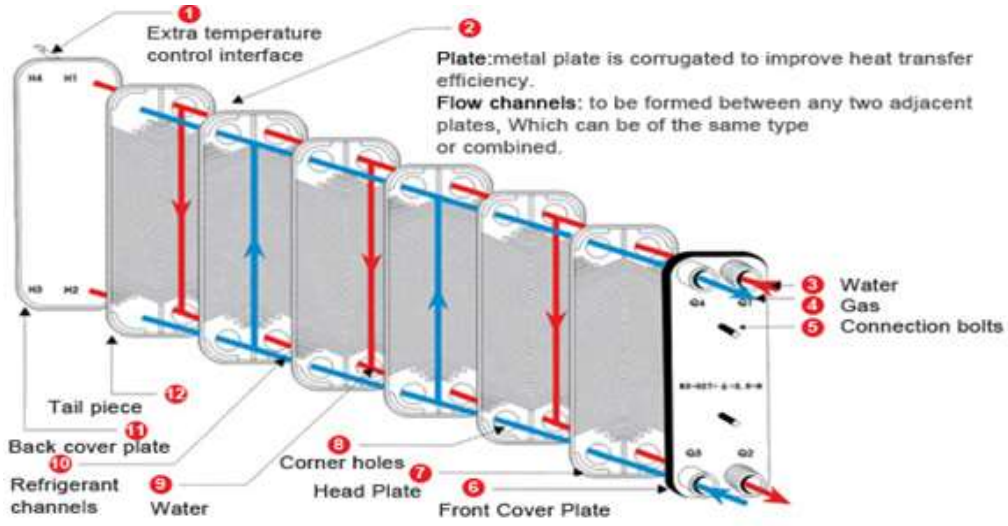

Figure 2.15: Plate type heat exchanger [W.14]

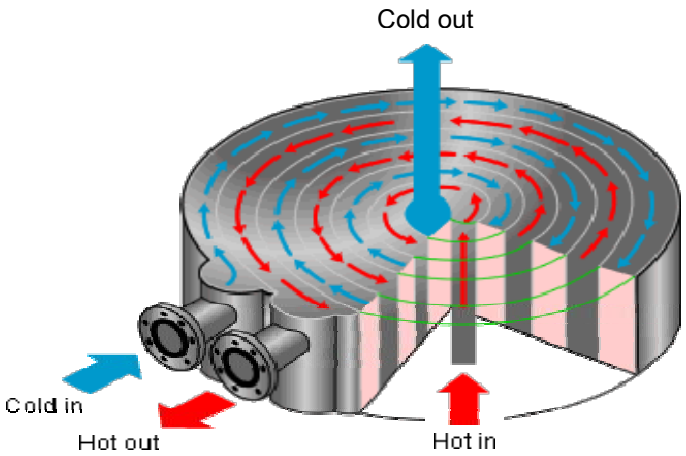

Figure 2.16: Spiral plate heat exchanger [W.11]

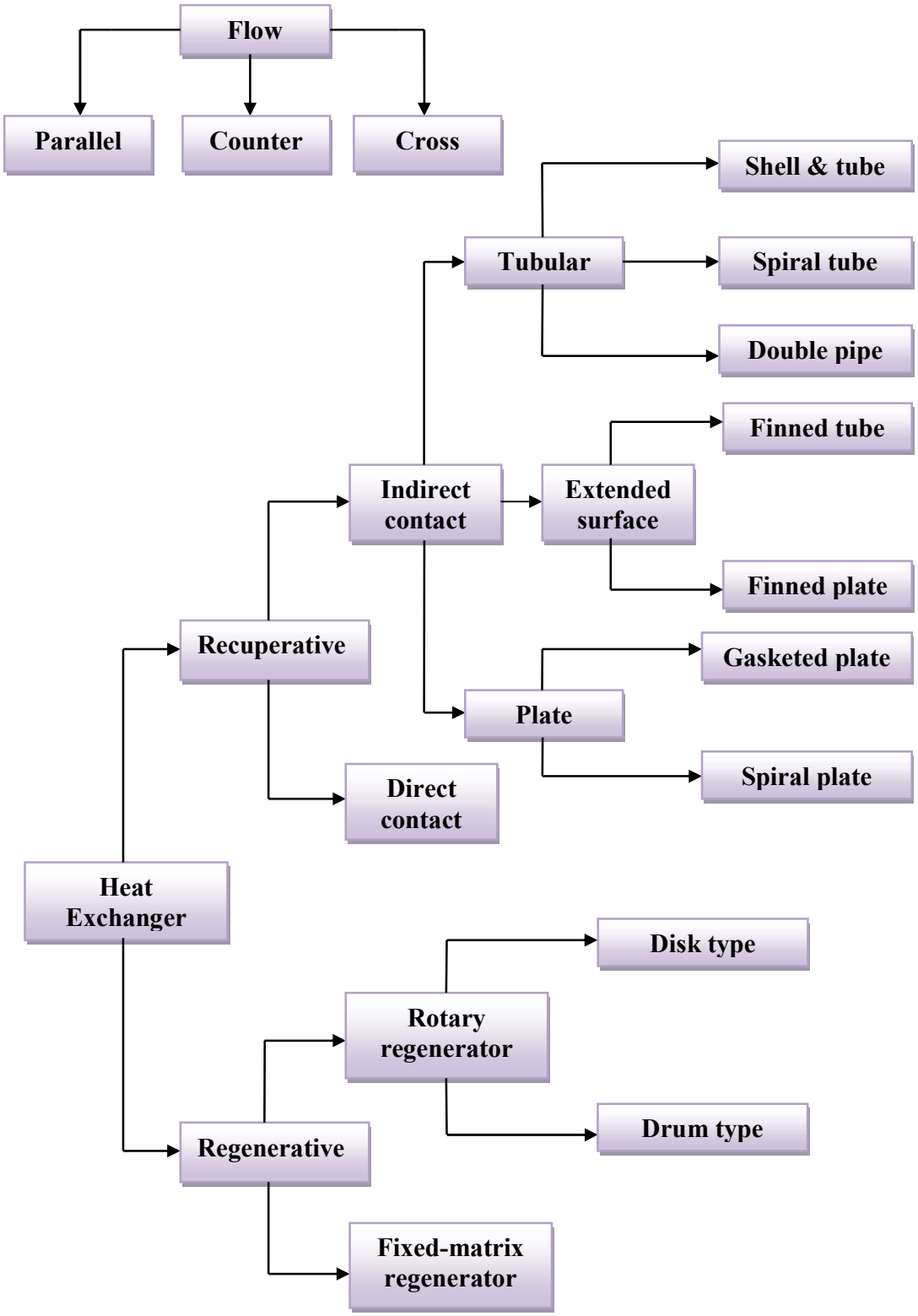

Figure 2.17: Classification of heat exchangers

2.7. Overall heat transfer coefficient

Cold and hot fluids are separated by a solid wall in indirect type heat exchangers. Heat is first transferred to the wall from the hot fluid by convection, through the wall by conduction, and to the cold fluid from the wall by convection. Overall heat transfer coefficient (U) is a parameter that takes into account all these modes of heat transfer. Sometimes, in the heat exchangers, an additional thermal resistance due to thin oxidation layer or crust deposit comes into account. This effect is taken into consideration through fouling resistance. More is the value of overall heat transfer coefficient, lesser will be the thermal resistance and more will be the heat transfer. The overall heat transfer coefficient and convective heat transfer coefficient has similar units *i.e.* W/m^2K.

For tubular heat exchangers, U is a function of heat transfer coefficients, tube diameter and appropriate fouling factors. Kakac [1991] provided a relation for overall heat transfer coefficient of a tubular heat exchanger without fins as given in Eq. (2.1).

$$\frac{1}{U} = \left(\frac{1}{h_i}\right) + FR_i + \left(\frac{d_i}{2K_t}\right) \ln\left(\frac{d_o}{d_i}\right) + \left(\frac{d_i}{d_o}\right) FR_o + \left(\frac{d_i}{d_o}\right)\left(\frac{1}{h_o}\right) \tag{2.1}$$

2.8. Logarithmic mean temperature difference

The temperature difference between the hot and cold fluids varies along the length of the heat exchanger. In any heat transfer analysis, the total rate of heat transfer (Q) is the quantity of primary interest and it is always better to have a mean temperature difference (ΔT_m) with heat transfer surface area (A_s) to be used in the equation of heat transfer *i.e.* Eq. (2.2).

$$Q = U \times A_s \times \Delta T_m \quad \text{or} \quad Q = U \times A_s \times LMTD \tag{2.2}$$

The average temperature difference between the hot and cold fluids is actually represented by the LMTD. This can be known by tracing the real temperature profiles of the fluid along the length of the heat exchanger. The exponential decay of the local temperature difference is truly reflected by LMTD. Over the entire length of the heat exchanger, the average temperature difference between the hot and the cold fluids is represented by Eq. (2.3).

$$\Delta T_m = \frac{\Delta T_i - \Delta T_o}{\ln\left(\frac{\Delta T_i}{\Delta T_o}\right)} \tag{2.3}$$

Where,

For parallel fluid flow:

$$\Delta T_i = \left(T_{h1} - T_{c1}\right) \tag{2.4}$$

$$\Delta T_o = \left(T_{h2} - T_{c2}\right) \tag{2.5}$$

For counter fluid flow:

$$\Delta T_i = \left(T_{h1} - T_{c2}\right) \tag{2.6}$$

$$\Delta T_o = \left(T_{h2} - T_{c1}\right) \tag{2.7}$$

Also, for a counter flow heat exchanger, when the capacity rates of hot and cold fluids are equal, the LMTD is indeterminate as in this case

$$\Delta T_i = \Delta T_o \text{ or } \left(T_{h1} - T_{h2}\right) = \left(T_{c2} - T_{c1}\right) \tag{2.8}$$

Therefore, for this special case, using L-Hospital's rule it can be shown that

$$\Delta T_m = \Delta T_i = \Delta T_o \tag{2.9}$$

It has been noted that for same inlet and outlet temperatures of the hot and cold fluids, the LMTD for counter flow exceeds than that for parallel flow type heat exchangers. Thus, for the required heat transfer rate, the heat transfer area required in case of counter fluid flow will be lesser than the area required for parallel flow regime [Kakac, 1991].

2.8.1. LMTD for multi pass heat exchangers

For multi pass heat exchangers, the LMTD defined in the above section is not valid. For such heat exchangers, a correction factor (C_f) comes into account and the net rate of heat transfer (Q) is represented by Eq. (2.10). The correction factor is a complex function of heat capacity rate ratio (R), temperature effectiveness (P) and the flow arrangement.

$$Q = C_f \times U \times A_s \times \Delta T_m \tag{2.10}$$

$$C_f = \Phi\left(R,\ P,\ \text{flow arrangement}\right) \tag{2.11}$$

$$R = \frac{\left(\text{Capacity rate}\right)_{cold}}{\left(\text{Capacity rate}\right)_{hot}} \tag{2.12}$$

$$P = \frac{\Delta T_{cold}}{\Delta T_{max}} \tag{2.13}$$

Knowing the flow arrangement, R and P, the value for 'C_f' can be found by using correction factor charts. Correction factor actually represents the degree of departure of the true mean temperature difference from the LMTD for a counter flow arrangement. For multi flow heat exchanges, the correction factor is always less than 1. The value of correction factor will be exactly 1 for a true counter flow heat exchanger [Kakac, 1991].

2.9. Fouling

Fouling may be defined as the accumulation of undesirable substances on the heat exchanger's surface. This collection and growth of unwanted material decreases the performance of heat exchangers. Due to fouling, an increase in heat transfer resistance, pressure drop and pumping power is generally observed which ultimately will decrease the effectiveness of the heat exchanger. Moreover, fouling results in enormous economic losses as initial cost and operation and maintenance cost are impacted by it.

Fouling also affects the design of a heat exchanger and for compensation, a fixed value as a fouling factor is generally provided during the design stage. This results in decrease in the overall heat transfer coefficient. Consequently, for the required heat transfer, excess surface area is provided to take up the loss in overall heat transfer coefficient. Charts given by TEMA are the most referred source for the fouling factor values [Kakac, 1991].

There are number of online and offline techniques currently available to control fouling. The heat exchanger surfaces can either be cleaned by using surface cleaning techniques like continuous and periodic cleaning or by the use of chemical additives. Different chemical additives acting as fouling inhibitors are usually used to minimize fouling depending upon the type of fouling *viz.* crystallization fouling, particulate fouling, biological fouling or corrosion fouling [Kakac, 1991].

2.10. Previous research work

The literature available on the application of waste heat recovery for purification of water is discussed in this section. Firstly, literature available on waste heat recovery, its quantity, advantages and different systems working on the basis of waste heat recovery are reviewed. The quality of drinking water in the '*Malwa'* region of Indian Punjab is very poor. Various concerned

reports and studies available are discussed in the later part. In the next part, waste heat recovery based water purification systems developed by various researchers are reviewed. The main objective of this work is to design a water purification unit working on the basis of waste heat of an IC engine; hence, literature available on the design of heat exchangers is also reviewed. Lastly, technological, economic and social issues concerning distillation and water purification are retrospected.

Saidur et al. [2012] reviewed the new technologies developed for recovery of the waste heat from IC engines. Various technologies like thermoelectric energy conversion using thermoelectric generators, Rankine bottoming cycle and turbocharging using exhaust waste heat were discussed. A relation between environmental impact, exergy efficiency and sustainability of a process was made. It was found that waste heat recovery based technologies are having large potential of energy savings. These technologies will help to improve engine efficiency. Also, with the advancement in exhaust waste heat recovery techniques, the surge in fossil fuel demand and greenhouse gas emissions can be restrained which will restrict global warming in the long run. Moreover, by using such technologies the emission of pollutants like SO_2 and NO_x will decline.

Pandiyarajan et al. [2011] conducted an investigation using finned shell and tube heat exchanger for exhaust waste heat recovery from diesel engine. The recovered heat was stored in a thermal storage medium. The experimental setup consisted of Kirloskar made four stroke, twin cylinder diesel engine having rated power 7.4 kW at 1500 rpm, an electrical dynamometer, finned shell and tube heat exchanger, and thermal storage system. Castor oil and paraffin were used as the sensible and latent heat storage mediums respectively. 320 grams of paraffin was filled in 48 cylindrical capsules having diameter of 80 mm and height 100 mm each and was kept in a thermal storage tank. A pump was used to maintain circulation of castor oil in the setup and thermocouples were used to record temperature at various locations. Uniform temperature was observed throughout the storage tank due to presence of stainless steel containers and high conductivity storage walls. Approximately, 10% – 15% of total heat was recovered by this system. The maximum heat recovered at full loading condition was 3.6 kW. Furthermore, an evaluation was made with respect to heat exchanger and storage tank's performance parameters

like amount of recovered heat, lost heat, rate of charging and charging efficiency. Results showed that the temperature of the exhaust gas can be decreased below 100 ^{o}C to recover more heat but this is possible only when there is no sulpher present in the exhaust gas. This may be due to the fact that by making the exhaust gas temperature below 100 ^{o}C the moisture present in the exhaust gas condenses and reacts with sulpher resulting in sulphonization which may corrode the heat exchanger tubes. Charging rate and charging efficiency were found to be increasing with load.

Bari and Hossain [2013] conducted experiments to check maximum obtainable waste heat from exhaust flue gas of a diesel engine. The experimental setup consisted of water cooled, four stroke and four cylinder diesel engine having rated torque 217 Nm at 2200 rpm, water dynamometer, fuel consumption meter, flow meter, thermocouples and pressure gauges. For this work, two heat exchangers were bought from the market. Water was used as a working fluid in the heat exchangers. It was found that waste heat recovery results in 16% additional power generation. Moreover, the heat exchangers used were not optimized for the respective application. So, certain changes were made to advance overall performance of the heat exchanging unit. Optimization was done with respect to the pressure of the working fluid and orientation of the heat exchangers. The additional power generation which was 16% before optimization changes to 23.7% after optimization.

Will [2012] analyzed the variations observed in simulation and test results for fuel conservation through lubrication system of an IC engine. It was noted that the lubrication system of these engines is having a large potential for emission reduction and fuel conservation. The analysis was done keeping in focus the water condensation effects and transfer of heat to the lubrication oil form the engine. Different configurations for recovery of the waste heat were developed. The results showed 7% reduction in fuel usage. The emission of pollutants like HC, CO and NO_x was also decreased by 2%, 27% and 19% respectively. In this work, a discussion was also made for benefits and risk of systems working on the principle of waste heat recovery. Furthermore, it was found that there are many benefits associated with these systems like reduction of wear in the engine, extension in the intervals of oil change and good performance of the engine.

He et al. [2011] improved the waste heat recovery from an IC engine by presenting a steady state experiment, exergy analysis and energy balance. The proposed thermodynamic cycle consisted of two cycles: the organic Rankine cycle, for recovering the waste heat of exhaust flue gas and lubricant; and the Kalina cycle, for waste heat recovery from the cooling system. The experimental setup consisted of Toyota made gasoline engine, eddy current dynamometer, rotameter, oil tank and temperature and flow measuring instruments. Suitable working fluids employed in high temperature organic Rankine cycle were also proposed by authors through thermodynamic analysis. The waste heat recovery using the proposed combined thermodynamic cycle was found to be more than the traditionally available cycles. However, this combined cycle was considered to be feasible only for naval engines because of its space requirement and complexity. Moreover, the cost associated with the combined cycle was also high due to addition of other components to be used in Kalina cycle.

Lee et al. [2010] studied effects of secondary combustion on efficiencies and reduction of emissions in the waste heat recovery system of a diesel engine. A secondary combustor consisting Nichrome wires in a ceramic cylinder was placed on the engine outlet so as to burn the un-burnt fuel leaving the diesel engine. Also, the heat from the exhaust gases and engine was recovered using fin-and-tube and shell-and-tube heat exchangers respectively. The experimental setup consisted of three cylinder and four cylinder 930 cc diesel engine, a 12 kW electric generator, a secondary combustor, and two heat exchangers for heat recovery. The amount of heat recovered was known from water temperature coming from the outlet of both heat exchangers. It was noticed that by performing secondary combustion and recovering heat through effective heat exchangers the thermal efficiency of the system increases by 20% – 25%. Moreover, due to this utilisation of waste heat, pollutants like NO_x, CO_x and particulate matter got reduced by 35%, 80% and 90% respectively. It was found that the amount of recoverable heat energy increases with electric power generation in the generator. A whole efficiency (electric power generation efficiency and thermal efficiency) of the system reached a value of 94.4% by recovering heat and performing secondary combustion.

Bajwa et al. [2015] investigated the distribution of heavy toxic elements and uranium in the drinking water samples collected from four districts of South – West Punjab namely Bathinda,

Mansa, Faridkot and Ferozepur. It was found that uranium accumulated in the liver, kidneys and the bones is having both radioactive and chemical effects. Uranium concentration in this region (called *'Malwa'*) was found to vary between 0.5 µg/l – 579 µg/l with an average of 73.5 µg/l. The permissible limits of uranium as per WHO and AERB are 30 µg/l and 60 µg/l respectively. Investigation results showed that out of total 498 samples analyzed, 68% surpass the safe limit given by WHO and 43% exceed the safe limit given by AERB. Also, it was noted that the concentration of heavy metals *viz.* As, Pb, Ni, Zn and Cr was above the safe limits given by WHO. These high concentrations might be due to natural geology, urbanization, industrial pollutants or large use of pesticides and fertilizers in this region.

Sekhon and Singh [2013] investigated the heavy metals concentration in water samples collected from tube wells of 100 different locations of the Patiala district of Punjab, India. For analysis, the technique of atomic absorption spectroscopy was used. Samples were analyzed for six different heavy metals *viz.* Ni, Se, Pb, Cr, Al and Cd. Then, samples were evaluated with respect to permissible limits defined by WHO. The content of Ni and Al was found to be quite high in most of the water samples but the content of other heavy metals like Se, Pb, Cr and Cd was lower than the WHO defined drinking water limits. According to the authors, poor solid waste management, anthropogenic and natural activities were the main reasons for water contamination.

Singh [2008] investigated the reason for cancer deaths in the *'Malwa'* region of Punjab, India. A significant correlation between cancer mortality with pesticides residue in soil and water was found. A correlation between cancer mortality and cropping pattern was also observed. Also, areas under cotton crop indicated a positive correlation with cancer mortality. The report confirmed that the use of pesticides and fertilizers to increase the yield from the agricultural fields is the biggest reason for cancer in the state of Punjab. It was also found that agricultural fires during the wheat season carries pesticides away with it causing health problems in the region. The report suggested that the Government of Punjab should take initiative to make Punjab, a pesticide free state and impose ban on agricultural fires. One cancer hospital should be built in the *'Malwa'* region of Punjab and water treatment plants (distillation units, ion exchange units or RO units) should be installed in all Punjab villages.

Mehra et al. [2007] studied the content of uranium in the water samples collected from the Malwa region of Indian Punjab using the technique of track etching. It was found that the content of uranium in the water samples taken from Burj Harike and Barnala ranges from 5.41 µg/l to 43.39 µg/l. These values were within safe limits defined by WHO and lower than the values noted in the water samples of Himachal Pradesh, India. The high content of uranium in some places might be due to the adjoining radioactive rich granites of Tusham Hills, Haryana.

Maheswari et al. [2015] conducted an experiment to desalinate water by using waste heat from exhaust of an IC engine. The experimental setup consisted of a four stroke, single cylinder, water cooled, 5 HP (at 1500 rpm) Kirloskar made diesel engine, an electrical dynamometer, and a distillation unit. The distillation unit was fitted in the path of exhaust flue gases. Submerged single pass evaporating unit, double pass water cooled condenser and a saline water storage tank were also present with the unit. The design of the evaporator and condenser was done using LMTD approach. It was found that the amount of desalinated water increases with preheating of the saline water coming to the evaporator. Also, with load, due to more heat produced during combustion, the exhaust gases gets heated up resulting in increased collection rate of distilled water. Fresh water collection rate by using water cooled condenser with preheating at maximum loading was found to be 3.0 LPH.

Tanaka and Park [2010] utilized thermal energy in the form of waste heat from a portable electric generator as a heat source for multiple-effect based diffusion solar still. A heat pipe was used for this purpose. The experimental setup as illustrated in Fig. 2.18 consisted of saline soaked wicks in the form of parallel partitions, condensing pipes, waste gas pipe and tanks for water collection. Distillate productivity was increased repeatedly through evaporation and condensation processes in the still. It was found that approximately half of the total thermal energy from waste gas of the generator can be given to the first partition of the solar still. Results indicated that about 20 kg of distilled water can be produced using this still at waste gas flow rates of 10, 20 and 40 m^3/h with an operation for 9, 5 and 3 hours respectively. The distillation water production rate was comparative to the maximum rate that can be obtained by using outdoor solar stills.

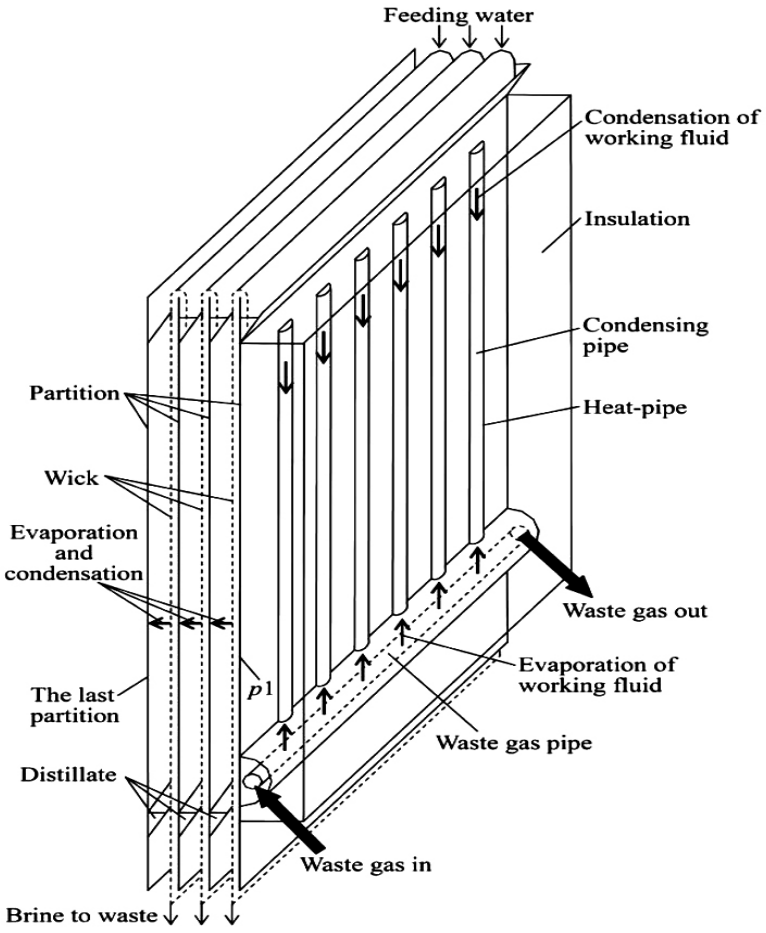

Figure 2.18: Distillation using waste heat of a portable electric generator [Tanaka and Park, 2010]

Sommariva [2008] utilized the waste heat from thermal power plant to optimize water production and performance ratio of multi-stage flash distillation and multi-effect distillation based plants. The heat from different process steams in the power plant was made available to the brine solution. Using this heat, the performance ratio of the distiller was also increased resulting in lesser fuel used for the supplementary firing. Also, through waste heat recovery, the environmental impacts of the desalinating plant also got reduced.

Moore et al. [2008] described an innovative water distillation system that uses sub-atmospheric pressure and hence low temperature was required to boil water. This system was working on the basis of Torricelli column principle which states that atmospheric pressure can bear a column of

water 10 m high and above this height the pressure will be very low. The experimental setup as shown in Fig. 2.19 consisted of two connected identical columns acting as evaporating and condensing units plus two pumps to pump saline water and fresh water. Saline water at a temperature higher than the fresh water was pumped to a height of 10 m. This water at sufficiently low pressure at the top vaporizes and flows through a pipe on top of the condenser and comes in contact with low temperature fresh water in the condensing unit, thus got condensed and was collected in the fresh water tank. The system can be used to produce any amount of water by varying the height of columns and by varying temperatures. The disadvantages with this system were the cost associated for heating purpose and the requirement of high capacity pumps for large applications.

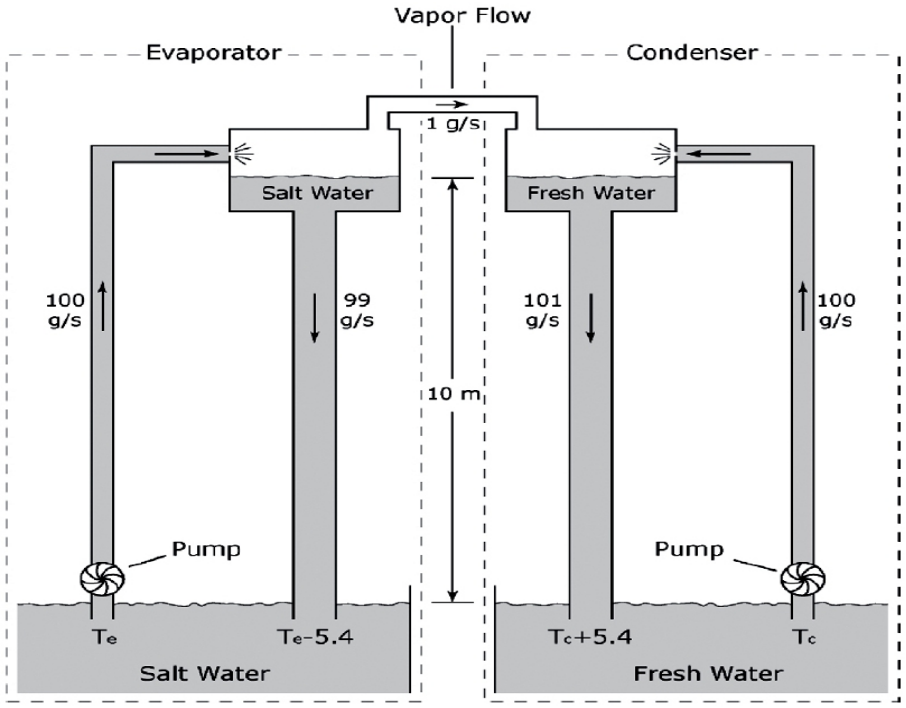

Figure 2.19: Torricelli principle based desalination unit [Moore et al., 2008]

Cardona et al. [2007] coupled a small sized thermal desalination system with a single-stage seawater RO system. The system was fed by a reciprocating natural gas engine. The heat was recovered from both cooling jacket water circuit and exhaust gas. The experimental setup as depicted in Fig. 2.20 consisted of a reciprocating natural gas engine, two heat exchangers, 12 effect based distillation unit of capacity 2000 m^3/day and a RO unit. Heat exchangers were

placed in series for extracting heat from cooling water jacket and exhaust gases. It was found that the feed water before entry to the RO system was having concentration of 38,000 ppm which reduced to 646 ppm after passing through the RO unit. This water was further mixed with distilled water coming from the distillation unit to obtain require quality water (TDS ≤ 500ppm, as defined by WHO) for drinking purpose. The advantages with this coupled system were reduced fresh water cost, less thermal pollution and significant power savings.

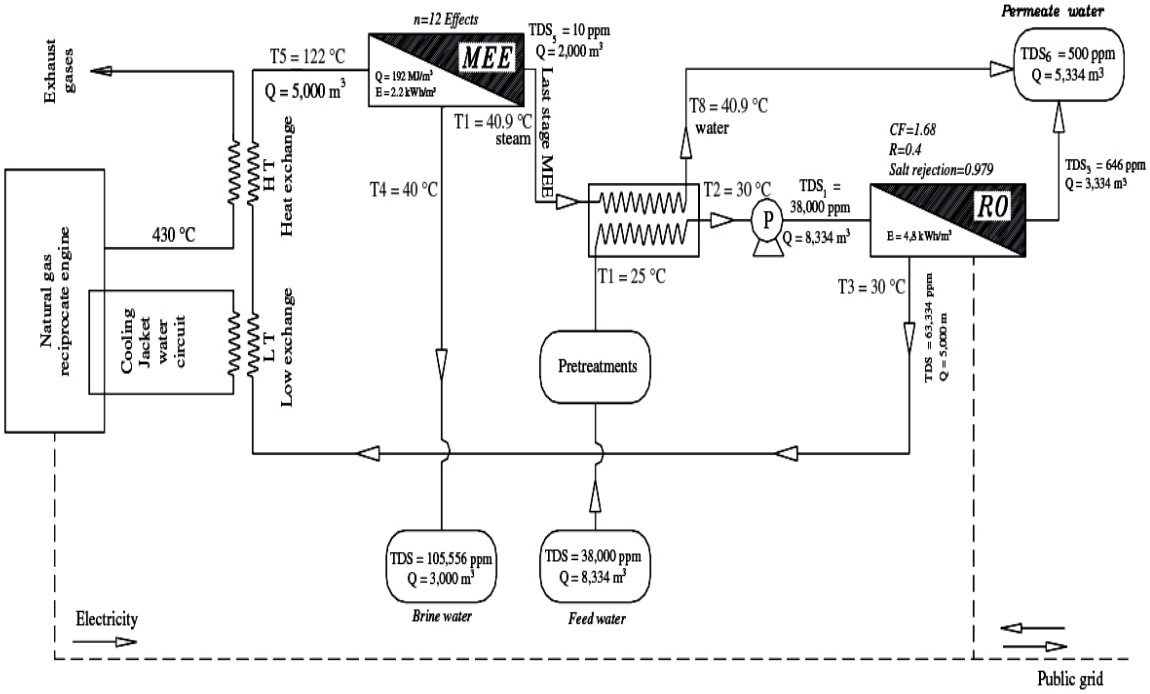

Figure 2.20: Desalination system coupled with a reciprocating engine [Cardona et al., 2007]

Rahman et al. [2003] carried experiments on a vertical tube submerged evaporator. The shell diameter and height of the evaporator was 400 mm and 500 mm respectively. The experimental set up consisted of an evaporator, chiller water tank, heating medium tank, feed water tank and a vacuum pump. In this experiment, the feed water was supplied by the feed water tank which flows vertically upwards inside the evaporator tubes and hot water from the heating medium tank flows on the shell side. Some feed water gets evaporated and was taken out by using the vacuum pump. Cooling water was continuously flowed for condensation of the vapors. Modeling and simulation were also performed for this system by assuming steady state conditions, one dimensional fluid flow inside the tubes and average properties. It was found that there was

increase in vapor generation with the surge in temperature of heating medium. However, by increasing the flow rate of feed water the vapor production has decreased due to reduction in the resident time. The fresh water production rate of this system was 144 kg/h. Hence, with this system, a fresh water quantity of 3.3 tons/day can be produced.

Kalogirou [2001] designed a low cost spray type evaporator in which the saline sea water was sprayed into fine droplets for evaporation of the water. The experimental set up as illustrated in Fig. 2.21 consisted of evaporating and condensing section, recirculation and seawater pumps, solar collector, and spraying nozzles. In this setup, seawater was pumped through the condensing unit which condenses the water vapors formed during spraying. The heat released from water vapors was given to the saline water which raises its temperature. The hot saline water was than passed through the solar collector where its temperature got raised. Finally, it was directed to nozzles for spraying action. The water collected at the bottom of the evaporating unit was directed to the solar collector where it was heated again and redirected to the nozzles for spraying action. In this system, a small number of heat exchangers made of carbon steel pipes were used which were placed mainly on the condensing unit side. Using this setup, the annual production with 1 m^2 of solar collector area was about 11.2 m^3.

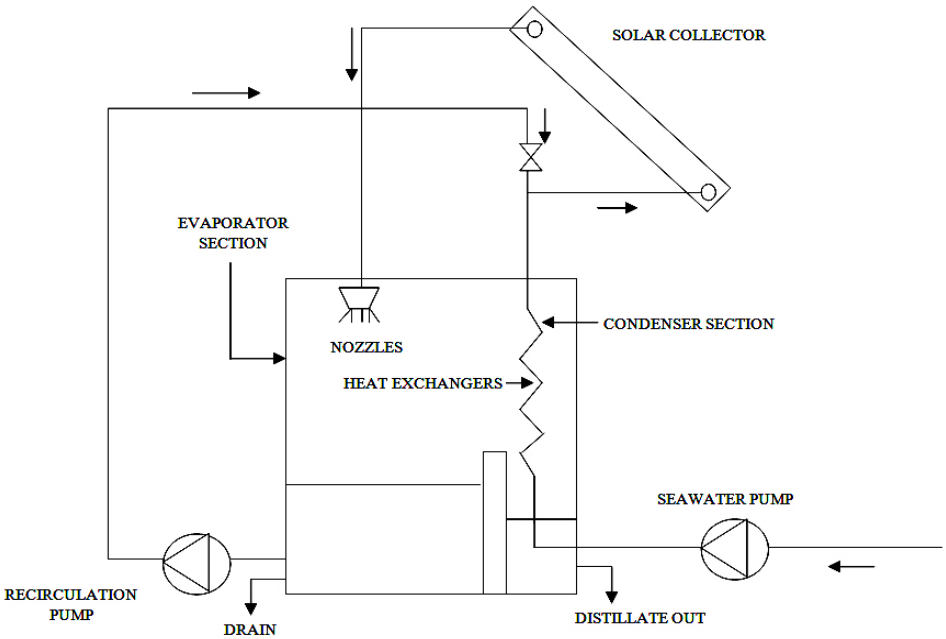

Figure 2.21: Desalination using spray type evaporator [Kalogirou, 2001]

Kundu [2015] designed a beneficial unbaffled shell-and-tube heat exchanger for connection of longitudinal fins with trapezoidal profile using parametric variation followed with Kern's method. In the experimental setup, two types of fin shapes rectangular and trapezoidal were longitudinally attached to the fin tubes. It was found that the rate of heat transfer increases and pressure drop decreases by using trapezoidal fins when the total volume of the fin over a tube was kept constant. This means that the heat transfer rates not only depend upon arrangement of tubes but it also depends upon the geometry of the fins.

Zhang et al. [2013] did heat transfer analysis of a finned-tube evaporator working on organic Rankine cycle for engine exhaust heat recovery using R245fa as a working fluid. The system consisted of a turbocharged diesel engine, finned tube counter flow evaporator, expander, generator, condenser and a pump. The evaporator was having three zones namely preheated, two phase and superheated zone. The working fluid after passing through the evaporator got expanded in an expander which further was linked to a generator. The evaporator was designed on the basis of LMTD method. It was found that exhaust gas mass flow rate increases slowly with engine load but rapidly with engine speed but the exhaust temperature follows reverse trend. Results showed that the mass flow rate of exhaust gas increases with engine power which in turn increases the overall heat exchange in the evaporator. The exhaust gas temperature was found to be decreasing as it passes through superheated zone – two phase zone – preheated zone. Additionally, preheated zone was found to have maximum heat transfer area followed by two phase zone and superheated zone.

Jamshidi et al. [2013] analyzed improvement of heat transfer in shell and helical tube heat exchangers. Effects of different fluid flow rates and geometrical parameters on heat exchange were found by using Taguchi method. The heat transfer coefficients on shell and tube side were noted using Wilson charts. The experimental setup consisted of copper made helical tubes having 10 turns with 9 mm inner diameter and 12.7 mm outer diameter. The shell was made of plexiglass having 14 cm inner and 15 cm outer diameters and having 25 cm length. Two parallel electric heaters having rated power 2000 W were used for heating water. The tube side fluid was hot water and shell side fluid was cold water. It was found that by raising coil diameter the Nusselt number increases and overall heat transfer coefficient also increases. The maximum heat

transfer rate was obtained by increasing the coil diameter, distance between two coils and mass flow rates of hot and cold fluids.

Markowski et al. [2013] investigated the influence of fouling on the recovery of heat in a network of shell-and-tube heat exchangers by assuming values for mass flow rate, inlet and outlet temperature and chemical composition for each process stream. Mathematical modeling was applied on the heat exchanger networks. It was found that by using the information collected from the past networks one can easily predict future changes and accordingly different methods can be employed to reduce fouling in the heat exchangers. A case study for optimal scheduling of cleaning interventions was also presented.

Pogiatzis et al. [2012] investigated two different methods available for cleaning of the heat exchangers which were subjected to both fouling and ageing. An approach was also made with respect to cleaning intervals of the heat exchangers. Authors found that ageing changes the soft gel formed due to fouling into more hard form known as coke. This coke can be removed by using one of the cleaning methods discussed but not by the other one. In this work, a process model in which ageing was considered by a simple two layer model was constructed using heat exchanger of counter-current type. It was noted that for cleaning process of heat exchangers, a combination of mechanical and chemical processes was superior to mechanical cleaning processes alone.

Faizal and Ahmed [2012] studied the rate of heat exchange and pressure drop in a corrugated plate heat exchanger with variable warm water flow rates and spacing. The corrugation on the plate surface induces turbulence which resulted in increasing the heat transfer rate which was found by help measuring temperature at the inlet and outlet of the plate heat exchanger. The experimental setup consisted of a corrugation pattern of 20 plates having heat transfer area 1.16298 m^2. Water was used both as a hot and cold fluid. It was found that overall heat transfer coefficient increases with increasing hot water flow rate for a given plate spacing. Also, the heat exchanger was found to be suitable with effective rate of heat transfer for plate spacing of 6 mm. Moreover, with corrugation, the net heat exchange has been increased. This work will be useful for the design of heat exchangers with small temperature difference applications.

Medrano et al. [2009] investigated the process of heat transfer of five small heat exchangers during charging and discharging. The heat exchangers were working as latent heat thermal storage systems. The experimental setup consists of five small heat exchangers, water pump, thermostatic bath, digital flow meter and different valves to control the flow rate of water. In one side of the heat exchanger, commercial paraffin RT35 acting as a phase change material was used. On the other side, water was circulated for the purpose of heat transfer. The studied heat exchangers were compared with the average thermal power values obtained for the comparison of average power per unit average temperature gradient and per unit area. The values were found to be highest in double pipe heat exchanger with graphite matrix based phase change material. However, average thermal power was found to be maximum in the compact type heat exchanger.

Wang et al. [2009] investigated enhancement of heat transfer of a shell-and-tube heat exchanger by installing sealers in the shell side placed in the gap between baffle plates and shell. Sealers were found to be cheap, easy to install, safe and long lasting. It was noted that three kinds of fluid flow modes exist in the heat exchanger's shell side. First, cross flow through the tube bundle than the flow through the gaps of segmental baffles and the last was shell-baffle leakage flow called short circuit flow. By installing sealers in the shell side, the short circuit flow was restricted and by doing so the fluid which earlier had not came in contact with the tube bundle for heat exchange now exchanges heat. So, by inserting sealers, the overall heat transfer rate has increased. Also, it was noted that by installing sealers, the heat transfer coefficient increased by 18.2 – 25.5% and the overall coefficient of heat transfer increased by 15.6 – 19.1%. Although the pressure losses surged by 44.6 – 44.8% with sealer installation yet the increased power consumption can be compensated by large increase in heat exchange which was far larger than the increased pumping power consumption. The sealers can be employed in new heat exchangers or can be installed in the existing installations easily.

Salimpour [2009] investigated coefficients of heat transfer of shell and helically coiled tube heat exchangers. For this study, three heat exchangers having varying pitches of coil were selected. Both counter flow and parallel flow configurations were used. 75 test runs were performed to calculate heat transfer coefficients for each test using fluid flow rates, plus inlet and outlet temperatures of shell-side and tube-side fluids. The experimental setup consisted of a centrifugal

pump, storage tank, an electrical heater, coiled tube heat exchanger, measuring pot, manometer, thermocouples and flow meter. In this work, empirical correlations were proposed for tube and shell side of the heat exchanger. A good agreement was found between the boundary layer based existing correlations and the calculated coefficients of heat transfer for tube side.

Kara and Güraras [2004] made a design model using the preliminary design of a shell-and-tube heat exchanger in which a single phase fluid was flowing on both tube and shell side. Initially, certain variables like type of working fluid, mass flow rates, fouling resistance, shell and tube material, along with inlet and outlet temperatures were needed to be provided by the operator. But, with the help of this program, the optimum area required for heat transfer, the complete dimensions of shell and tube bundle were determined keeping minimum possible pressure drop. Furthermore, best heat exchanger was selected from 240 heat exchangers using this program. Moreover, this program can be extended to different heat exchanger configurations like multiple tube passes. The program was flexible to introduce other working fluids in place of water.

Lattemann and Hopner [2008] studied the impacts of seawater desalination on environment. It was found that desalination is used to resolve the issue of potable water scarcity in coastal areas. Desalination systems are having both advantages and disadvantages. Some of the negative impacts are concentrate and chemical discharges, energy demand and danger to the marine life. Also, it is required that a proper disposal system should be made for concentrate and chemical discharges. Desalination systems working on the basis of renewable energy sources like solar, wind, biomass or on waste heat recovery from stationary engines, power plants etc. should be designed in the future.

Khawaji et al. [2008] reviewed the status and technological advancements in the area of seawater desalination. 75 million people in the World obtain fresh water by the desalination of brackish water or seawater. Authors noted that the multi stage flash distillation and reverse osmosis are the two main techniques used mostly for the purpose of desalination. Further research and development with respect to economic aspects, water cogeneration systems, solar energy based desalination systems, RO membranes and resulting concentrate treatment will decrease the production cost of desalinated water.

Karagiannis and Soldatos [2008] reviewed various water desalination methods with respect to the economic aspects. It was found that the production cost of fresh water through desalination depends on many factors like salinity in the feed water, type of energy source, method adopted for desalination and total capacity of the desalinating plant. The production cost of fresh water using conventional energy systems ranges from 0.4 €/m^3 to 3 €/m^3. Using renewable energy sources, it can be as high as 15 €/m^3. Although production cost was found to be much higher using renewable energy systems yet it can be compensated by lower gas emissions and environmental benefits. Authors found that there are two methods available for desalinating water *viz.* membrane processes (mainly reverse osmosis) and thermal processes (like multistage flash distillation and multi-effect distillation). Membrane processes are used by medium and low capacity systems, while thermal methods, are used in medium and large capacity systems. *IPSEpro*, *RESYSpro* and *AUDESSY* are some of the software tools developed for ecological, economic and technical analysis of water desalination methods.

Chapter 3

Objectives

The studies conducted by Bajwa et al. [2015], Sekhon and Singh [2013], Tripathi et al. [2013], Singh [2008] and Mehra et al. [2007] found that the content of physico-chemical parameters, heavy metals and uranium is quite high in the Malwa belt of Punjab, India. Although, in the past, much work has been done in the area of desalination yet there is no work done to remove physico-chemical parameters and heavy metals present in the drinking water. Following are the set objectives of the proposed thesis work:

i. To find the amount of heat energy present in the exhaust flue gas of an IC engine that can be made available to perform distillation of groundwater at varying loads and compression ratios, plus designing and fabrication of water purification unit on the basis of maximum recoverable heat.

ii. To collect drinking water samples from hand pumps of four different locations *viz*. Kotkapura, Faridkot, Sri Muktsar Sahib and Bathinda in the *'Malwa'* region of Indian Punjab, and perform tests for the presence of physico-chemical parameters (TDS, conductivity and pH) and heavy metals (Zn, Pb, Fe, Co and Cr) in them.

iii. To perform distillation of groundwater using the designed water purification unit and calculate the distilled water collection rate at varying loads and compression ratios.

iv. To test the collected distilled water for the presence of physico-chemical parameters and heavy metals.

v. To compare purity levels of obtained distilled water and RO water and finding out the payback period of the proposed distillation unit at different working conditions.

Chapter 4

Methodology and experimentation

The main objective of this chapter is to design evaporating and condensing unit for the water purification unit on the basis of maximum recoverable waste heat from variable compression ratio engine. The chapter will also provide the details of experimental setup, instrumentation and operational procedure. At the end, details of the region from where drinking water samples were collected are given.

4.1. Recoverable waste heat

The amount of heat energy that can be recovered from exhaust gas of an IC engine varies with the compression ratio, load, speed and capacity of the engine. With the engine speed remaining constant, the quantity of recoverable heat energy changes only with the compression ratio and load. Experiments were performed at Internal Combustion Laboratory of Thapar University, Patiala at four different compression ratios – 12:1, 14:1, 16:1 and 18:1. The load on the engine was varied from 2 to 10 kg using eddy current dynamometer having arm length 185 mm.

A stand alone panel having air box, manometer, fuel tank, and fuel and air flow measuring devices was present with the engine. Analog signals recorded from various locations of the engine were sent to data acquisition software 'Enginesoft' for online performance evaluation.

Variation of exhaust gas mass flow rate with load on the engine is depicted in Fig. 4.1. It can be seen that the mass flow rate of exhaust gas increases with increase in load on the engine. A surge is also observed with compression ratio which is possible because of increase in the swept volume of the engine with compression ratio, which results in more exhaust mass flow rate at higher compression ratios. Figure 4.2 illustrates the variation of exhaust flue gas temperature at the inlet of the calorimeter unit with load on the engine. An increase is seen in temperature of the exhaust flue gas with load. This may have become possible due to increased amount of fuel injection at higher loads, resulting in more heat generation and thus the increase in temperature. The temperature is more prominent at lower compression ratios because at higher compression ratios, due to more expansion, swept volume increases because of which air intake into the

engine increases, resulting in comparatively low exhaust gas temperature than the temperature at lower compression ratio.

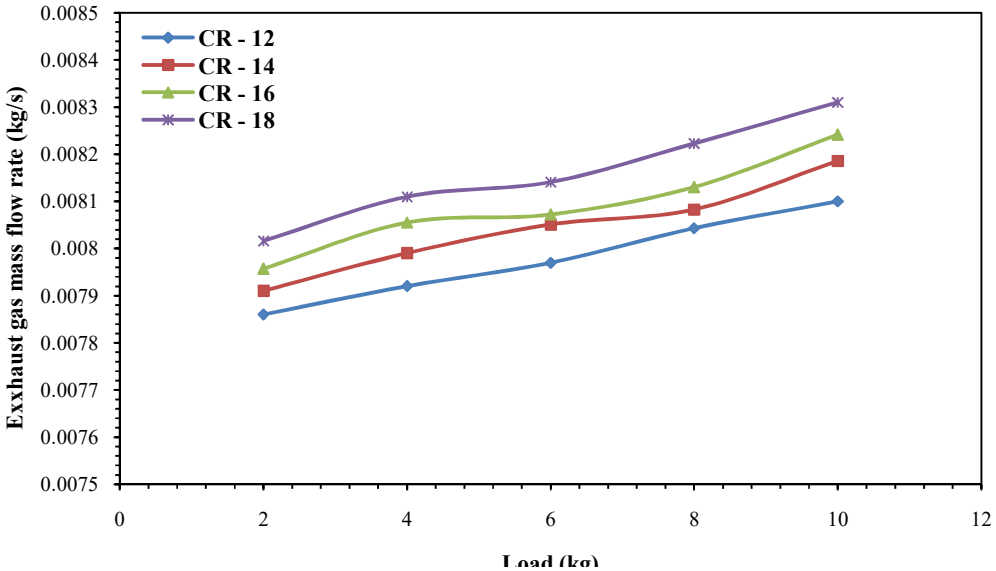

Figure 4.1: Variation of exhaust gas mass flow rate with load on the engine

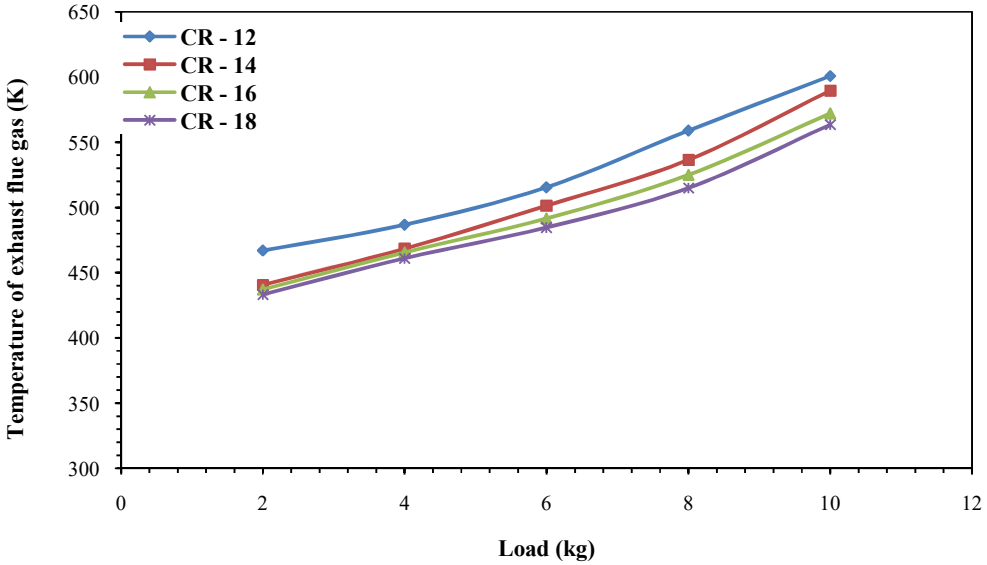

Figure 4.2: Variation of exhaust flue gas temperature with load on the engine

The amount of heat that can be extracted from exhaust flue gas at different loads was calculated by using Eq. (4.1)

$$Q_e = \dot{m}_e \times C_e \times (T_{ei} - T_{eo}) \quad (4.1)$$

Figure 4.3 shows the variation of maximum extractable heat from exhaust flue gas with load on the engine. Temperature at outlet of the evaporator unit was considered to be ambient for calculation of the maximum heat. The maximum extractable heat noted was 2.43 kW at 12:1 compression ratio and 10 kg load.

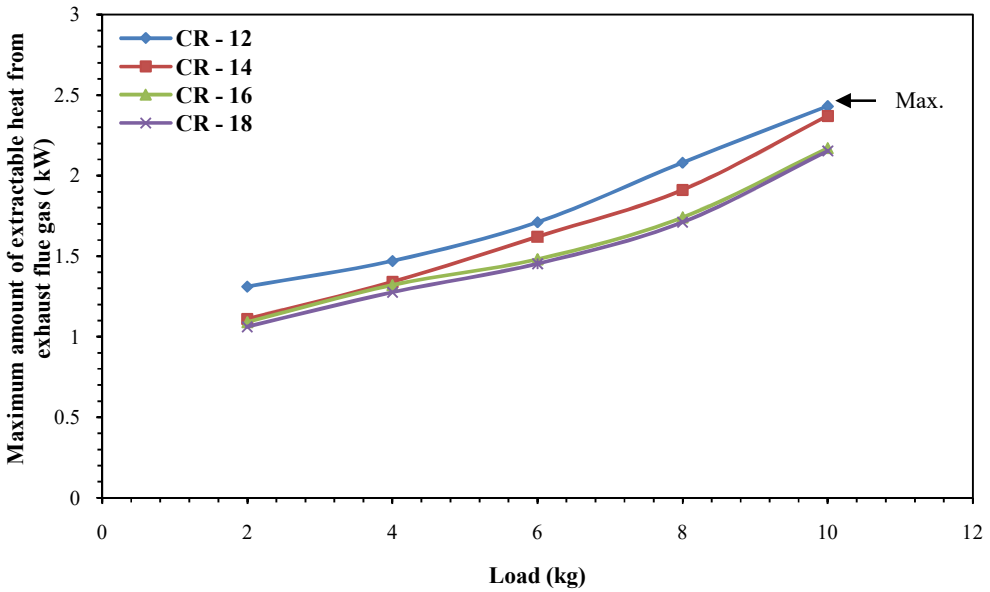

Figure 4.3: Variation of maximum extractable heat with load on the engine

However, ambient temperature can never be considered as the flue gas temperature at the outlet of evaporator, due to two following reasons:

i. Both sulfur and water droplets are present in the flue gas. Due to the ambient conditions at the outlet of the evaporator, the water droplets get condensed resulting in formation of the sulphuric acid which may result in corrosion of the evaporator tubes made up of copper.

ii. The temperature of the exhaust gas should always remain higher than 100 ^{o}C as it is passing through the water which is at boiling temperature under atmospheric conditions.

Due to these reasons, the temperature at outlet of the evaporator was considered to be more than 100 ^{o}C *i.e.* 120 ^{o}C. Figure 4.4 indicates the variation of actual extractable heat from exhaust flue gas by considering this temperature at the outlet of evaporating unit. Now, maximum actual extractable heat noted was 1.68 kW at compression ratio 12:1 and 10 kg load.

Temperature and fluid flow measurements were taken 30 minutes after the engine has been started to obtain stable readings.

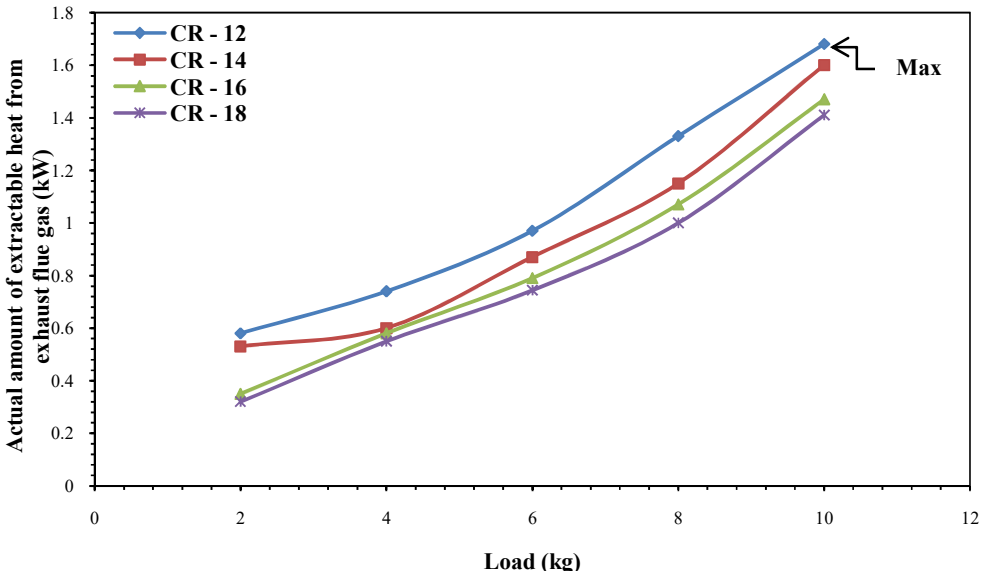

Figure 4.4: Variation of actual extractable heat with load on the engine

4.2. Design of the heat exchangers

Rating and sizing problems are the most common heat exchanger design problems. Rating problems are used to find out the temperatures and rates of fluid flow at the outlet of the heat exchanger when surface area of heat transfer and dimensions of the flow passage are available. However, sizing problems are used to find out the heat exchanger area, type of construction, flow arrangement, and shell and tube material to satisfy the requirements like hot and cold fluid inlet temperatures, rate of heat transfer and pressure drop. If the temperatures at the inlet condition, one of the temperatures at the outlet condition and mass flow rate of hot and cold fluids are given, than LMTD method can be employed to find out the total heat transfer area by using following five steps [Kakac, 1991]:

Step – 1: Calculate the heat transfer rate and one unknown outlet temperature.

Step – 2: Calculate the LMTD and if necessary obtain the correction factor (C).

Step – 3: Calculate the overall heat transfer coefficient.

Step – 4: Determine the total heat transfer area.

Step – 5: Decide tube diameter, tube length, number of tubes, tube layout, tube pitch and shell diameter.

4.2.1. Evaporator design

A single pass horizontal tube submerged evaporator (HTSE) was designed to avoid any performance loss of the engine due to restriction in the exhaust gas flow. The evaporator was designed by considering exhaust gas temperature at the outlet of the evaporator to be 120 ^{o}C. Also, an additional space to collect water vapors was needed in the evaporating unit. So, the copper tubes were fixed at the bottom of the evaporator making it a submerged type evaporator. The LMTD method was used for the designing purpose. Kakac [1991] proposed the following assumptions for the heat exchanger design:

i. Evaporator is operating under steady state conditions.
ii. Heat generation in the evaporator is zero.
iii. Evaporator is an adiabatic system *i.e.* no heat transfer to the surroundings.
iv. For each fluid, specific heat at constant pressure remains constant throughout the operation.
v. There is no heat conduction longitudinally in the wall and fluid.
vi. If one of the fluid streams changes phase, it is considered to be occurring at a constant pressure and temperature.
vii. The overall heat transfer coefficient remains constant all the way through the evaporator including in the case of phase change.
viii. The temperature of the fluids (hot and cold) is uniform over every cross-section of flow.

The amount of heat that can be extracted from exhaust flue gas at different loads in this recovery unit was calculated by using Eq. (4.2)

$$Q_e = \dot{m}_e \times C_e \times \left(T_{ei} - T_{eo}\right) \tag{4.2}$$

Here, the value for specific heat capacity of the exhaust flue gas was taken to be 1.21 kJ/kgK [W.8]. The maximum amount of actual extractable waste heat was found to be 1.68 kW. Both sensible and latent heats were needed for the distillation of water from atmospheric conditions. So, under atmospheric conditions, heat required for distillation of water is given by Eq. (4.3) in which C_{gw} and L_{gw} were assigned values 4.18 kJ/kgK [W.20] and 2257 kJ/kg respectively.

$$Q_r = \left(\dot{m}_{gw} \times C_{gw} \times \left(\Delta T_{gw}\right)\right) + \left(\dot{m}_{gw} \times L_{gw}\right) \quad (4.3)$$

As per first law of Thermodynamics,

Heat energy lost by exhaust gases = heat energy gained by surrounding ground water

$$\dot{m}_e \times C_e \times \left(T_{ei} - T_{eo}\right) = \left(\dot{m}_{gw} \times C_{gw} \times \left(\Delta T_{gw}\right)\right) + \left(\dot{m}_{gw} \times L_{gw}\right) = \dot{m}_{st} \times L_{st} \quad (4.4)$$

For equal capacity rate of hot and cold fluids, area of heat transfer and number of tubes in the evaporator were found on the basis of heat energy estimation given in Eq. (4.5).

$$Q_e = U_{oe} \times A_{he} \times \left(\Delta T_{lme}\right) = U_{oe} \times A_{he} \times \left(T_g - T_{bw}\right) \quad (4.5)$$

Where,

i. U_{oe} is the overall heat transfer coefficient for the evaporator which takes into account all three heat transfer modes plus internal and external thermal and fouling resistances. It was calculated by using the equation below [Kakac, 1991]:

$$\frac{1}{U_{oe}} = \left(\frac{1}{h_{ei}}\right) + FR_{ei} + \left(\frac{d_{ei}}{2K'}\right) \ln\left(\frac{d_{eo}}{d_{ei}}\right) + \left(\frac{d_{ei}}{d_{eo}}\right) FR_{eo} + \left(\frac{d_{ei}}{d_{eo}}\right)\left(\frac{1}{h_{eo}}\right) \quad (4.6)$$

In which,

a. h_{ei} is the evaporator inside heat transfer coefficient which was found by using Eq. 4.7 called Dittus-Boelter's equation. This equation was applied considering fully developed turbulent flow inside the evaporator tubes. It gives a relation between Nusselt number (Nu_e), Reynolds number (Re_e) and Prandtl number (Pr_e).

$$Nu_e = 0.023 \left(Re_e\right)^{0.8} \left(Pr_e\right)^{0.3} \quad (4.7)$$

The exponent of Prandtl number here was considered to be 0.3 as exhaust flue gas in the evaporator tubes was undergoing cooling.

- $Re_e = \frac{\rho_e \times V_e \times d_{ei}}{\mu_e}$, $\rho_e = 0.405$ kg/m^3 [W.8] (4.8)

- $Pr_e = \frac{\mu_e \times C_e}{K_e}$, $K_e = 0.0466$ W/m.K [W.3], $\mu_e = 37.9 \times 10^{-6}$ Pa.s [W.8] (4.9)

- Also, $Nu_e = \frac{h_{ei} \times d_{ei}}{K_e}$ (4.10)

b. FR_{ei} = Fouling resistance at the inside of evaporator = 0.001761 m^{2}K/W [Kakac, 1991].

c. FR_{eo} = Fouling resistance at the outside of evaporator = 0.000176 m^{2}K/W [Kakac, 1991].

d. d_{ei} and d_{eo} are the internal and external diameters of the evaporator tubes which were considered to be 12 mm and 14 mm respectively.

e. Copper was considered to be used as an evaporator tube material due to its good thermal conductivity (K' = 370 W/mK), easy availability and low cost.

Area of the evaporating unit was found by using Eq. (4.11).

$$A_{he} = \frac{Q_e}{U_{oe} \times \left(T_g - T_{bw}\right)} = \pi \times d_{eo} \times l_e \times N_e \tag{4.11}$$

Number of evaporator tubes was calculated from

$$N_e = \frac{A_{he}}{\pi \times d_{eo} \times l_e} \tag{4.12}$$

To find the number of tubes, the diameter and length of the evaporator tubes were considered in accordance with the market availability than the hit and trail method was used to find out the number of tubes with respect to the required heat transfer rate. Only single pass tubes were considered in the design because multi pass tubes may increase pressure drop across the evaporator. Also, for submerged design, multi pass tube design was not a viable option.

Tubes having internal diameter 12 mm were placed in triangular pitch pattern. Tube pitch for this layout was found to be 18 mm [Kakac, 1991]. On the basis of number of tubes, tubes pitch and pitch ratio, the diameter of the shell was found. Mild steel was used for making the shell of the evaporator because of its malleable and ductile nature, low thermal conductivity, easy availability and lower cost. The specifications of the evaporating unit are shown in Table 4.1. Front view and cross-sectional side view of the evaporator (with dimensions in mm) are shown in Fig. 4.5 and Fig. 4.6 respectively. Figure 4.7 (a) and (b) depict Pro-E models of the evaporating unit.

Table 4.1: Specifications of the evaporating unit

Name of the component	Dimensions	Material used
Internal diameter of the evaporator tubes (d_{ei})	0.012 m	Copper
External diameter of the evaporator tubes (d_{eo})	0.014 m	Copper
Length of the evaporator tubes (l_e)	0.50 m	Copper
Number of tubes/passes	07/01	-
Diameter of the evaporator shell (d_{esi})	0.140 m	Mild steel
Length of the evaporator shell (l_{es})	0.780 m	Mild steel

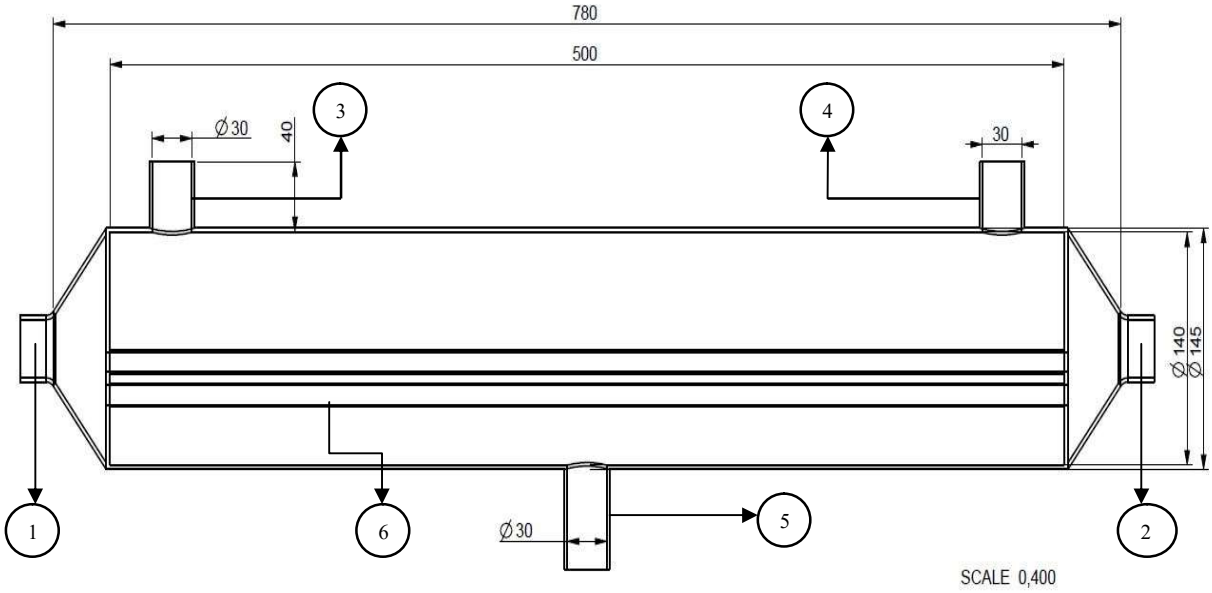

1 – Exhaust flue gas inlet	2 – Exhaust flue gas outlet	3 – Steam outlet
4 – Ground water inlet	5 – Drain valve	6 – Evaporator tubes

Figure 4.5: Front view of the evaporator

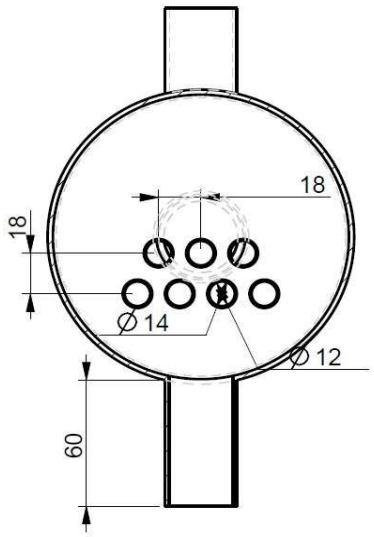

Figure 4.6: Cross-sectional side view of the evaporator

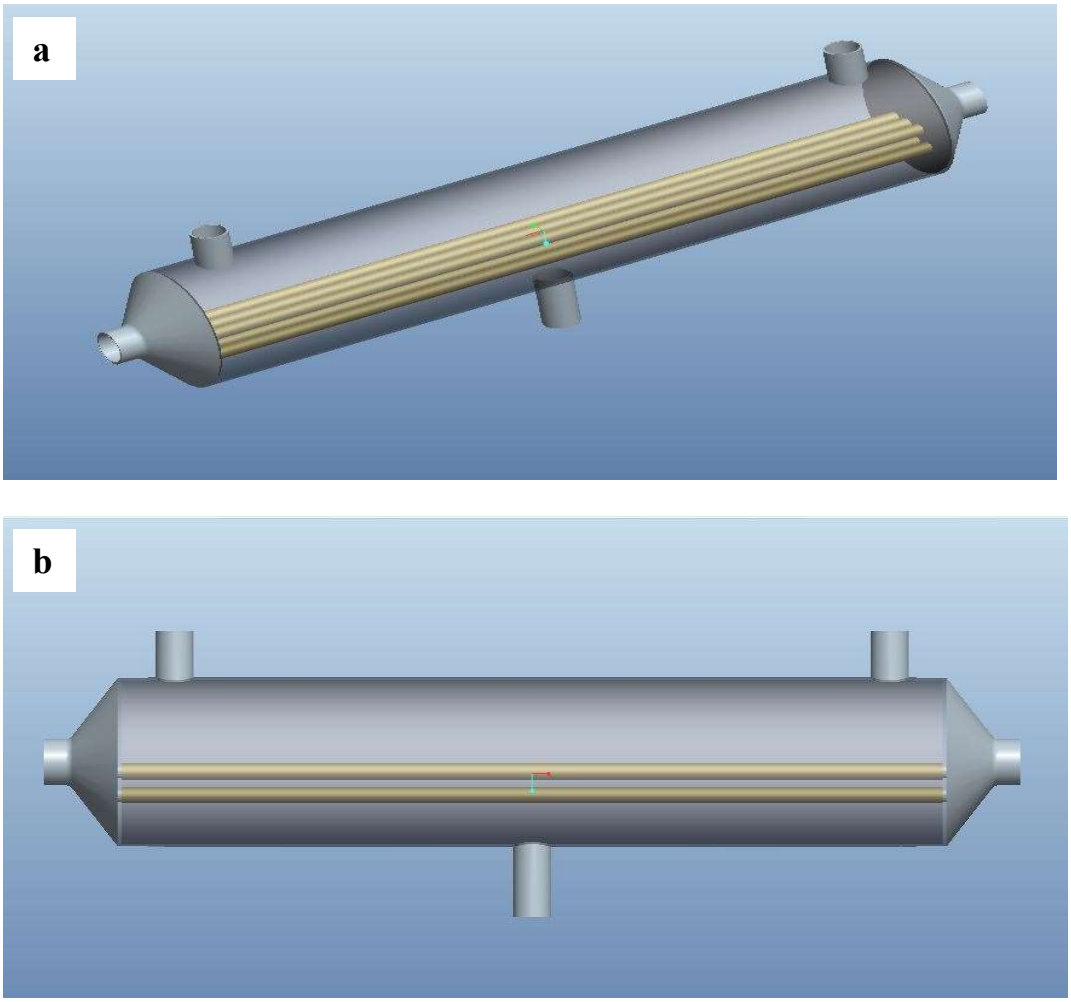

Figure 4.7 (a) and (b): Pro-E models of the evaporator

4.2.2. Condenser design

The steam formed in the evaporator was passed through the water cooled condenser where its condensation takes place. In the condenser, ground water was used to take up the heat from the steam and distilled water formed was collected in the distilled water storage tank. Ground water after taking up the heat from the steam was passed to the hot ground water storage tank. The condensing unit was designed on the basis of evaporation rate. The design was based upon LMTD method and following were the assumptions made:

i. Condenser is operating under steady state conditions.

ii. Heat generation in the condenser is zero.

iii. Condenser is an adiabatic system *i.e.* no heat transfer to the surroundings.

iv. For each fluid, specific heat at constant pressure remains constant throughout the operation.

v. There is no heat conduction longitudinally in the wall and fluid.

vi. If one of the fluid streams changes phase, it is considered to be occurring at a constant pressure and temperature.

vii. The overall heat transfer coefficient remains constant all the way through the evaporator including in the case of phase change.

viii. The temperature of the fluids (hot and cold) is uniform over all cross-sections of flow.

Heat load on the condenser was calculated by using Eq. (4.13).

$$Q_c = \dot{m}_{st} \times \left(h_{fg} - h_f\right) \tag{4.13}$$

As per first law of Thermodynamics,

Heat energy released by the water vapors = heat energy absorbed by surrounding ground water

$$\dot{m}_{st} \times L_{st} = \left(\dot{m}_{dw} \times C_d \times \left(\Delta T_{dw}\right)\right) + \left(\dot{m}_{gw} \times C_{gw} \times \left(T_{gwo} - T_{gwi}\right)\right),\ L_{st} = 2257 \text{ kJ/kg} \tag{4.14}$$

Here, C_d and C_{gw} were assigned values of 4.22 kJ/kgK and 4.18 kJ/kgK respectively [W.20].

Area of heat transfer and number of tubes of the condenser were found on the basis of energy estimation given below in Eq. (4.15).

$$Q_c = C_c \times U_{oc} \times A_{hc} \times \left(\Delta T_{lmc}\right) \tag{4.15}$$

Where,

i. C_c is the correction factor which is a function of heat capacity rate ratio (R), temperature effectiveness (P) and the flow arrangement.

- $$C_c = \Phi\left(R,\ P,\ \text{flow arrangement}\right) \tag{4.16}$$
- $$R = \frac{\left(\text{Capacity rate}\right)_{cold}}{\left(\text{Capacity rate}\right)_{hot}} = \frac{T_{dwi} - T_{dwo}}{T_{gwi} - T_{gwo}} \tag{4.17}$$
- $$P = \frac{T_{gwo} - T_{gwi}}{T_{dwi} - T_{gwi}} \tag{4.18}$$

Knowing the flow arrangement, R and P, the value for 'C_c' was found by using correction factor charts and it comes out to be 0.61 [Kakac, 1991].

ii. ΔT_{lmc} is the logarithmic mean temperature difference for condenser which was determined by using the following equation

$$\Delta T_{lmc} = \frac{\Delta T_i - \Delta T_o}{\ln\left(\Delta T_i / \Delta T_o\right)} = \frac{\left(T_{dwi} - T_{gwo}\right) - \left(T_{dwo} - T_{gwi}\right)}{\ln\left(\frac{\left(T_{dwi} - T_{gwo}\right)}{\left(T_{dwo} - T_{gwi}\right)}\right)} \quad (4.19)$$

iii. U_{oc} is the overall heat transfer coefficient for the condenser which can be calculated by using the equation given below

$$\frac{1}{U_{oc}} = \left(\frac{1}{h_{ci}}\right) + FR_{ci} + \left(\frac{d_{ci}}{2K'}\right)\ln\left(\frac{d_{co}}{d_{ci}}\right) + \left(\frac{d_{ci}}{d_{co}}\right)FR_{co} + \left(\frac{d_{ci}}{d_{co}}\right)\left(\frac{1}{h_{co}}\right) \quad (4.20)$$

In which,

a. h_{ci} is the condenser inside heat transfer coefficient which was found by using Dittus-Boelter's equation (considering fully developed turbulent flow inside the condenser tubes). It gives a relation between Nusselt number (Nu_c), Reynolds number (Re_c) and Prandtl number (Pr_c).

- $Nu_c = 0.023\left(Re_c\right)^{0.8}\left(Pr_c\right)^{0.4}$ (4.21)
- $Re_c = \frac{\rho_c \times V_c \times d_{ci}}{\mu_c}$, $\rho_c = 988$ kg/m3 [W.20], $\mu_c = 547.1 \times 10^{-6}$ Pa.s [W.15] (4.22)
- $Pr_c = \frac{\mu_c \times C_{gw}}{K_{gw}}$, $K_{gw} = 0.58$ W/mK [W.13] (4.23)
- Also, $Nu_c = \frac{h_{ci} \times d_{ci}}{K_{gw}}$ (4.24)

b. FR_{ci} = Fouling resistance at the inside of condenser = 0.000176 m^2K/W [Kakac, 1991].

c. FR_{co} = Fouling resistance at the outside of condenser = 0.000088 m^2K/W [Kakac, 1991].

d. d_{ci} and d_{co} are the internal and external diameters of the condenser tubes which were considered to be 12 mm and 14 mm respectively.

e. Condenser tubes were considered to be made up of copper having conductivity 370 W/mK.

The heat transfer area of the condenser is calculated by

$$A_{hc} = \frac{Q_c}{C_c \times U_{oc} \times \Delta T_{lmc}} = \pi \times d_{co} \times l_c \times N_c \quad (4.25)$$

The condenser tube length can be calculated from

$$l_c = \frac{A_{hc}}{\pi \times d_{co} \times N_c} \tag{4.26}$$

To find the number of tubes, the diameter and length of the condenser tubes were considered in accordance with the market availability than the hit and trail method was used to find out the number of tubes with respect to the required rate of heat transfer. For making the size of the condenser small and for better heat transfer a two pass copper tube was used.

Using number of tubes and number of passes, the diameter of the condenser shell was calculated. Mild steel was used for making the shell of the condenser. The specifications of the condensing unit are shown in Table 4.2. Front view and cross-sectional side view of the condenser (with dimensions in mm) are shown in Fig. 4.9 and Fig. 4.10 respectively. Pro-E models of the condensing unit are illustrated in Fig. 4.11 and Fig. 4.12.

Table 4.2: Specifications of the condensing unit

Name of the component	Dimensions	Material used
Internal diameter of the condenser tube (d_{ci})	0.012 m	Copper
External diameter of the condenser tube (d_{co})	0.014 m	Copper
Total length of the condenser tube (l_c)	0.58 m	Copper
Number of tubes/passes	01/02	-
Diameter of the condenser shell (d_{csi})	0.096 m	Mild steel
Length of the condenser shell (l_{cs})	0.380 m	Mild steel

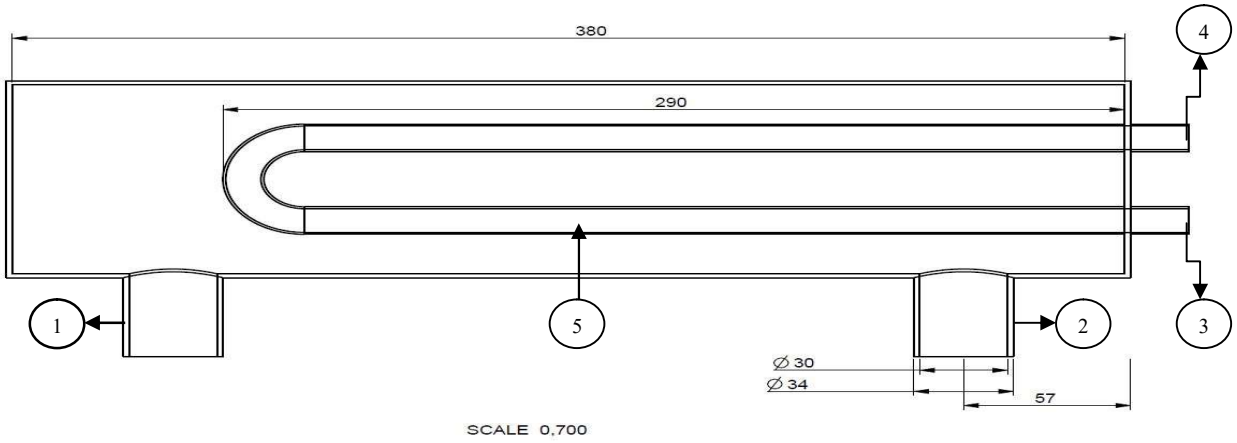

1 – Distilled water outlet 2- Steam inlet 3 – Fresh ground water inlet

4 – Preheated ground water 5 – Condenser tube

Figure 4.8: Front view of the condenser

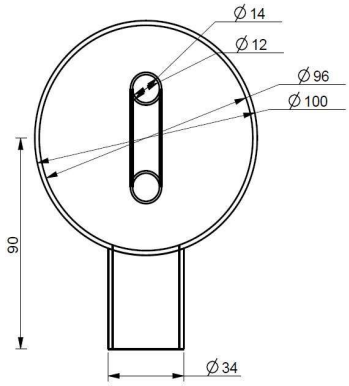

Figure 4.9: Cross-sectional side view of the condenser

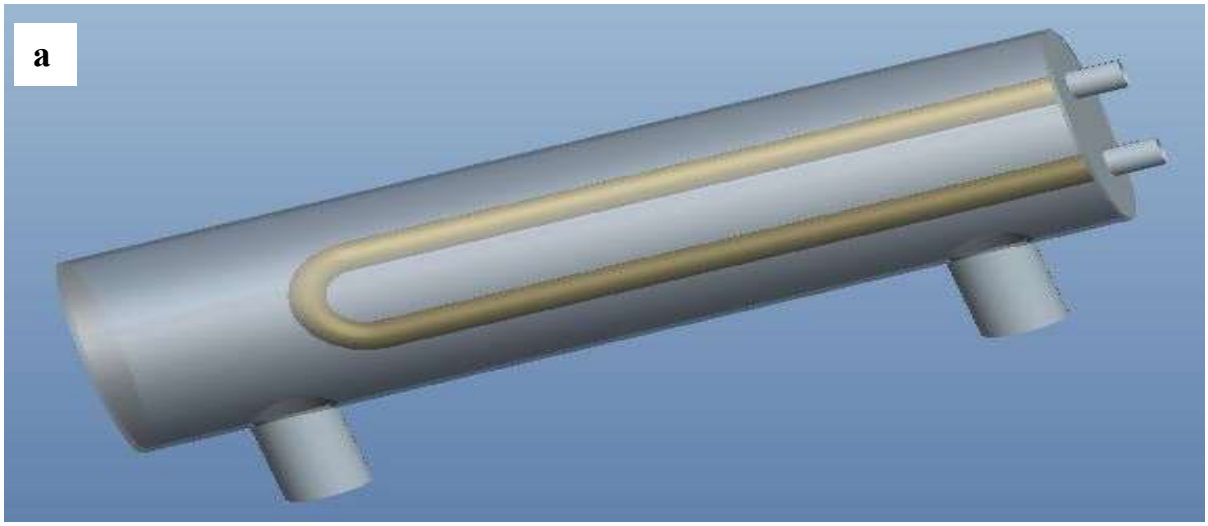

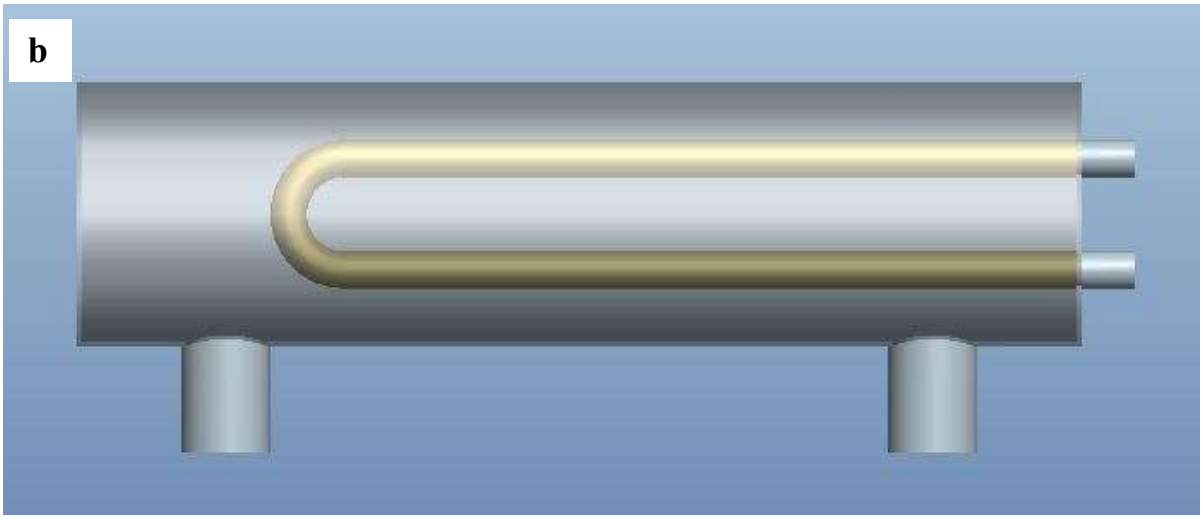

4.10 (a) and (b): Pro-E models of the condenser

4.3. Experimental setup

4.3.1. System operation

The calorimeter unit integrated initially with the engine was disengaged. In place of this, an exhaust waste heat recovery unit was assembled in the exhaust gas path of variable compression ratio engine. The schematic arrangement of the experimental setup is illustrated in Fig. 4.11. The heat recovery unit consists of a shell-and-tube single pass evaporator, made up of mild steel and copper respectively. The tube side fluid in this heat exchanger was exhaust flue gas and shell side fluid was ground water.

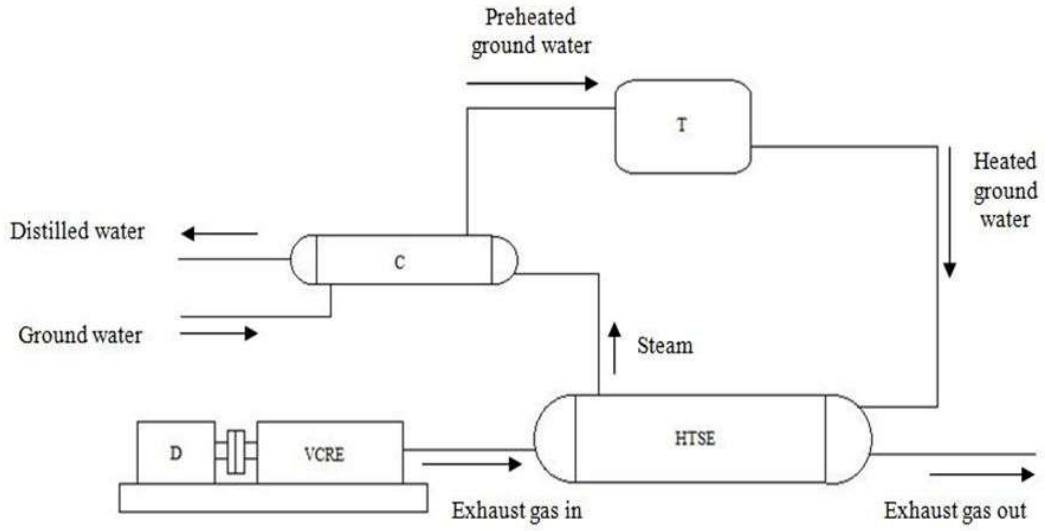

D – Eddy current dynamometer VCRE – Variable compression ratio engine C – Water cooled condenser
HTSE – Horizontal tube submerged evaporator T – Hot ground water storage tank

Figure 4.11: Schematic arrangement of the experimental setup

The preheated ground water from the ground water storage tank was fed to the evaporating unit. The supply of ground water to the evaporator was controlled by using ball control valve. In the waste heat recovery unit, heat from the exhaust flue gas was transferred to the surrounding ground water resulting in evaporation of ground water and steam so formed was passed through the stainless steel wire braided flexible pipe into the double pass shell-and-tube water cooled condenser, where the energy from the steam was taken by the flowing ground water

resulting in condensation of the steam. Distilled water formed due to this condensation process was collected in the distilled water storage tank. The hot ground water from the condenser was stored in the storage tank. A drain valve for suitable drainage and other measuring instruments were provided in the evaporating unit. Photographs of the experimental setup and water purification unit are depicted in Fig. 4.12 and Fig. 4.13 respectively.

Figure 4.12: Photograph of the experimental setup

Figure 4.13: Photograph of the water purification unit

4.3.2. Components of the system

i. Variable compression ratio engine

Distillation of ground water was performed at the internal combustion engine (ICE) Laboratory of Thapar University, Patiala. For this work, exhaust waste heat of an IC engine was used. The engine used was a single cylinder and four stroke variable compression ratio diesel engine. The specifications of the engine are given in Table 4.3. In this engine, compression ratio (CR) can be varied easily with the help of tilting cylinder block arrangement. The loosening or fastening of six Allen key bolts and one lock nut changes the distance between top dead centre (TDC) and bottom dead centre (BDC) due to which swept volume of the engine changes. Hence, compression ratio changes with respect to Eq. (4.27). Figure 4.14 and Fig. 4.15 depict VCRE and mechanism to change compression ratio respectively.

$$\frac{V_{sw}}{V_{cl}} = CR - 1 \tag{4.27}$$

The load on the engine was varied from 2 to 10 kg using bi-directional water cooled eddy current dynamometer having arm length 185 mm. This dynamometer works on the basis of Faraday's law of magnetic induction. For load measurement, strain gauge load cell was used. The shaft of the dynamometer moves across a magnetic field which produces movement resistance on the shaft resulting in load variations. The engine was integrated with the exhaust waste heat recovery unit for the purpose of water purification.

Table 4.3: Specifications of the VCRE

Make	Kirloskar
Model	TV1
Type	Four stroke
Number of cylinders	Single
Cylinder bore	87.5 mm
Stroke length	110 mm
Connecting rod length	234 mm
Rated power	3.5 kW at 1500 rpm
Compression ratio range	12 – 18
Swept volume	661.45 cc
Cooling type	Water cooling

Figure 4.14: Variable compression ratio diesel engine
[ICE Laboratory, Thapar University, Patiala]

Figure 4.15: Mechanism to change compression ratio of VCRE

ii. Horizontal tube submerged evaporator

A horizontal tube submerged evaporator was designed for the purpose of waste heat recovery from exhaust flue gas. The evaporator was a shell-and-tube type heat exchanger having seven copper tubes inside it. The shell of the evaporator was made up of mild steed. Hot ground water coming from the storage tank into this unit takes heat from the outgoing exhaust gas and gets evaporated, forming steam which further was condensed to form distilled water in the condenser. The evaporator and flue gas piping systems were well insulated by mineral wool having thermal conductivity 0.04 W/m^{o}C and reflective aluminum cladding to avoid heat losses to the ambient environment. Figure 4.16 demonstrates the evaporating unit. The inlet and outlet temperatures of the exhaust flue gas passing through the evaporator were measured using K type thermocouples. A drain valve was also provided in the evaporator for cleaning purpose.

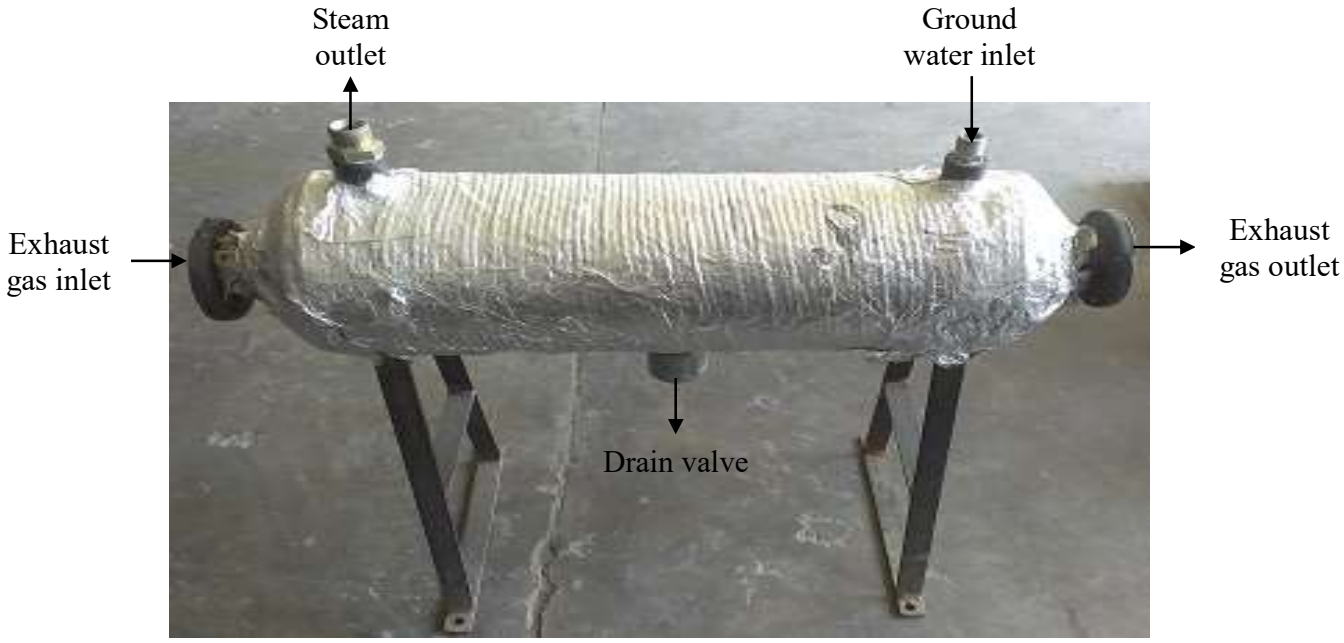

Figure 4.16: Evaporating unit after insulation and aluminum cladding

iii. Water cooled condenser

A two pass, single tube, shell-and-tube heat exchanger was designed for the condensation of the steam coming from the evaporator. The fresh ground water in the tube side takes up the heat from the steam resulting in condensation. Finally, distilled water was obtained in the distilled water storage tank. It was found to be fit for drinking purpose after mineralization. Ground water

after taking the heat from the steam was passed to the hot ground water storage tank. Condenser is shown in Fig. 4.17.

Figure 4.17: Water cooled condensing unit

iv. Piping for water purification unit

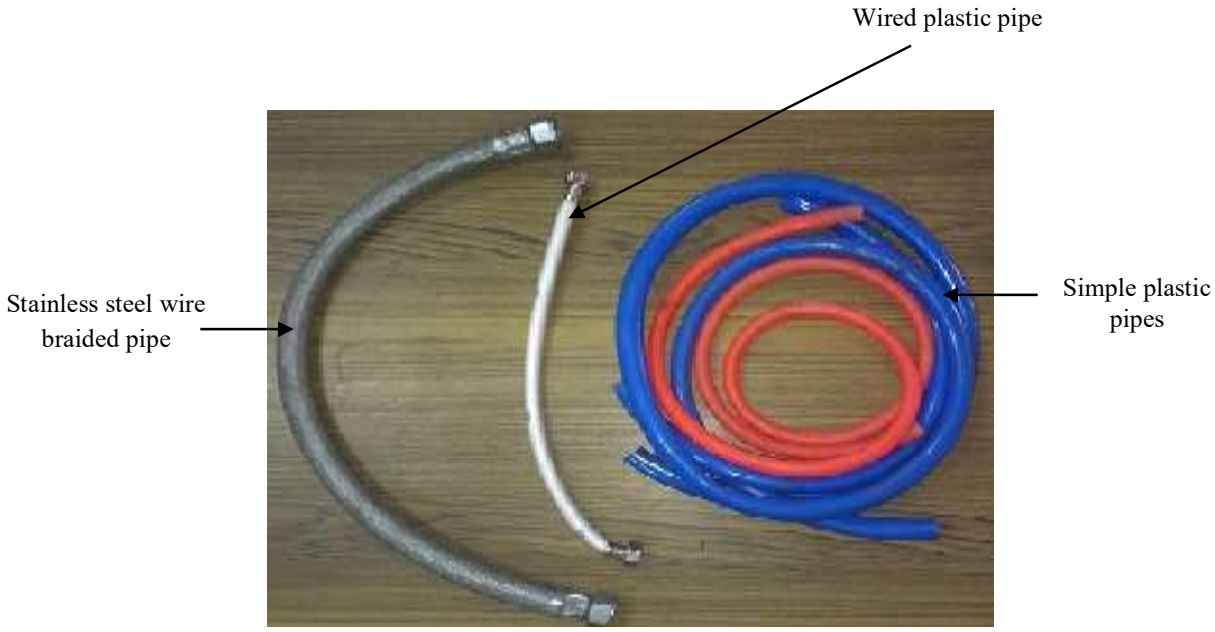

Figure 4.18: Different type of pipes used for conveying steam and water

Pipes made up of different materials were used to supply steam and water to various locations in the water purification unit. The temperature of the steam leaving the evaporator unit was quite high, and simple plastic pipe cannot serve the steam conveying purpose. So, stainless steel wire braided flexible pipe was used. The preheated water from the storage tank was supplied to the evaporator through a wired plastic pipe. In addition to this, simple plastic pipes were used to transfer fresh ground water to the condenser unit for condensation of steam, and preheated ground water from the condenser unit to the hot water storage tank. Different pipes used for conveying steam and water in the unit are shown in Fig. 4.18.

v. Hot ground water storage tank

Hot ground water after taking up the heat from the steam in the condensing unit was passed through pipe to the hot ground water storage tank. This tank was used as a reservoir to store the preheated ground water. It was fitted with ball type control valve which ensures the controlled supply (3 LPH) of preheated ground water to the evaporator where its distillation will take place. The tank was made up of mild steel and its dimensions were 0.30 m × 0.30 m × 0.30 m with a total volume of 0.027 m^3. Also, the tank was made rust free by coating it with paint. Figure 4.19 shows the storage tank used in the experimentation

Figure 4.19: Hot ground water storage tank

vi. Distilled water storage tank

The steam formed in the evaporating unit got condensed in the condenser resulting in the formation of distilled water. This distilled water was collected in the distilled water storage tank. The plastic tank with dimensions 0.15 m × 0.15 m × 0.15 m and volume 0.00675 m^3 was used as a storage tank. The tank was thoroughly cleaned before experimentation to remove any contaminates initially present. Volume of collected distilled water can be found by measuring the height of water in this tank. Figure 4.20 shows the distilled water storage tank**.**

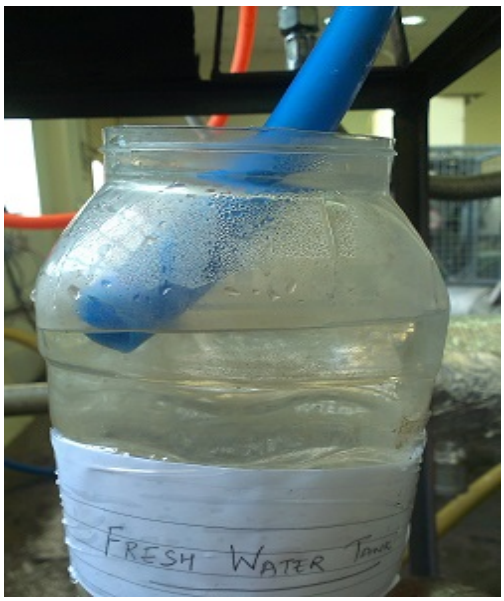

Figure 4.20: Distilled water storage tank

4.3.3. Measuring Instruments

i. Stand alone panel box and sensors

A stand alone panel box as shown in Fig. 4.21 consisting of air box, manometer, fuel tank, fuel measuring unit, fuel and air flow measuring devices, digital voltmeter, load indicator and piezo powering unit was present with the system. Also, a 'Eureka' made rotameter is installed for cooling water flow measurement. Piezo sensor and K type thermocouples were used for the pressure and temperature measurement respectively. Figure 4.22 depicts piezo sensor. Online performance of the engine was evaluated using engine performance analysis software package 'Enginesoft'.

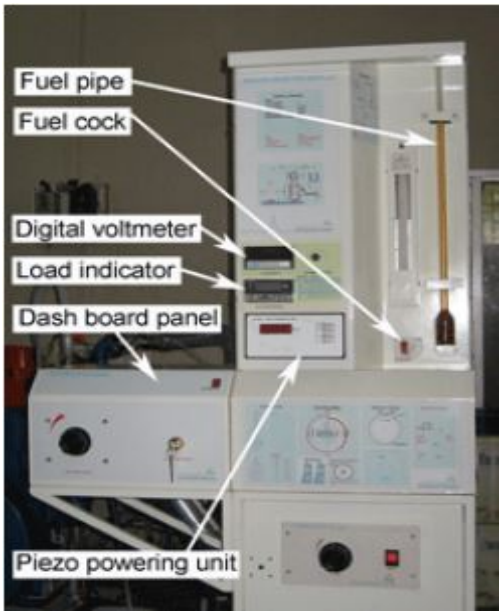

Figure 4.21: Stand alone panel box

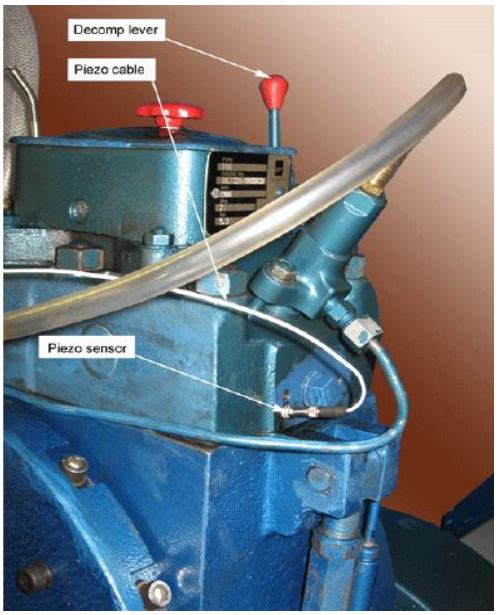

Figure 4.22: Piezo sensor

ii. TDS meter

HM digital made TDS-3 meter was used to check total dissolved solids present in given water sample. The TDS meter used is shown in Fig. 4.23. The accuracy and TDS range of this meter were ± 2% and 0 – 9990 ppm respectively. It can work in the temperature range of 0 ^{o}C – 80 ^{o}C. The average conversion factor (NaCl based) to convert TDS into electrical conductivity for this meter was 2.

Figure 4.23: HM Digital made TDS meter [Energy laboratory, Thapar University, Patiala]

iii. pH measuring instrument

Water can be checked for its acidic or alkaline nature by checking its pH. It was measured by using Spectralab made Eco pH meter. Initially, the calibration of the instrument was done by

dipping the pH electrode into 7 pH buffer solution. The accuracy and pH range of this meter were 0.02pH/0.1mV and 0.0 – 14 pH. It can work in temperature range of 0 ^{o}C – 99 ^{o}C. The pH meter used in the experiment is shown in Fig. 4.24.

Figure 4.24: Spectralab made pH meter [Energy laboratory, Thapar University, Patiala]

iv. Microwave Plasma Atomic Emission Spectrometer (MP-AES)

The water samples collected from different locations were tested for the content of heavy metals (Zn, Pb, Fe, Co and Cr) using Agilent made 4100 MP-AES system. This system works on the principle of atomic emission spectroscopy (AES). The MP-AES system is shown in Fig. 4.25.

Figure 4.25: MP-AES apparatus [SAI Laboratories, Thapar University, Patiala]

v. Thermometer

Figure 4.26 shows mercury-in glass thermometers used for the measurement of temperature at various positions of the water purification unit. The measuring range of these thermometers was from -10 ^{o}C to 100 ^{o}C.

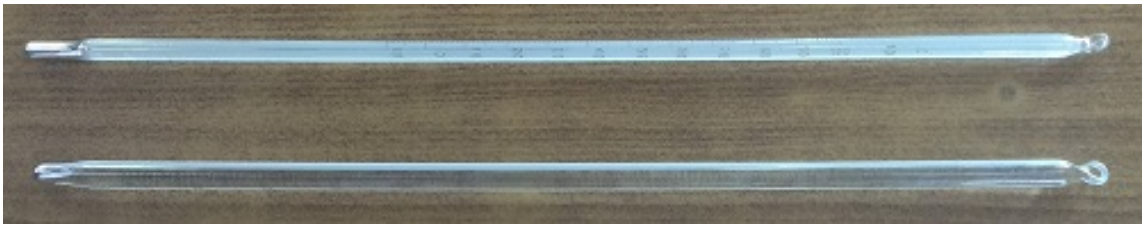

Figure 4.26: Mercury-in glass thermometers [RAC Laboratory, Thapar University, Patiala]

4.4. Collection of water samples

For this investigation, four drinking water samples were collected from Kotkapura, Faridkot, Sri Muktsar Sahib and Bathinda which fall in Punjab's agricultural heartland – the *'Malwa'* region. Punjab is a northwestern state of Republic of India having a total area of 50,362 km^2. Agriculture is the main source of income for most of the people of the '*Malwa*' region. The study region is depicted in Fig. 4.27. Table 4.4 provides details of the study region. As per studies conducted by Bajwa et al. [2015], Sekhon and Singh [2013], Tripathi et al. [2013], Singh [2008] and Mehra et al. [2007], the content of heavy metals and uranium is quite high in these areas. About one liter of water sample was initially collected for analysis purpose from the hand pumps of each location in the month of February, 2016. Many people used to drink water from hand pumps in these locations. Following are the guidelines followed for the purpose of sampling [W.18].

i. A polyethylene bottle was used for collecting samples.
ii. The bottle used for the sampling process was sufficiently cleaned.
iii. The bottle was rinsed three times with the sample before it is filled.
iv. Two samples were collected from each location.
v. The collected samples were labeled with marker about the location and date of collection.
vi. A small air gap was left in the bottle so that sample can be thoroughly mixed at the time of analysis.
vii. After collection, samples were stored in the refrigerator.

viii. For better results, the time between sampling and analysis was kept minimum possible.

Study region

- Faridkot (1475 sq. km)
- Sri Muktsar Sahib (2593 sq. km.)
- Bathinda (3367 sq. km.)

Figure 4.27: Map of Punjab, India showing study region [W.7]

Table 4.4: Details of the study region [W.6, W.10]

Serial no.	District	Area (Sq. km)	Population	Coordinates	Main source of drinking water (%age of households)					
					Tap water		Hand pump/bore well		Other sources	
					R	U	R	U	R	U
01.	Faridkot^	1475.7	617508	30.6782° N, 74.7396° E	33.9	55	62.6	42.3	3.5	2.7
02.	Sri Muktsar Sahib	2593	901896	30.2391° N, 74.4995° E	53.1	58.8	42.9	39.5	4	1.7
03.	Bathinda	3367	1388525	30.1252° N, 74.0611° E	47.4	74.2	48.2	24.2	4.4	1.6

^ Kotkapura is in district Faridkot
R – Rural areas
U – Urban areas

After collecting samples, the analysis was done for physico-chemical parameters and content of heavy metals. Physico-chemical parameters like TDS, conductivity and pH were measured respectively by using TDS-3 and Eco pH meter. For the content of heavy metals (Zn, Pb, Fe, Co and Cr), the MP-AES system was used

Chapter 5

Results and discussion

The water samples collected from four different locations of the *'Malwa'* region of Punjab, India were tested for the presence of physico-chemical parameters and heavy metals (Zn, Pb, Fe, Co and Cr). The results of the analysis and reasons behind the high concentration of TDS and heavy metals in drinking water samples are presented in this chapter. A comparison between distilled and RO water with respect to the physico-chemical parameters and content of heavy metals is also given. Finally, a discussion is made for the approximate total cost of the proposed water purification unit and payback period at different working conditions.

5.1. Tests before distillation

5.1.1. Physico-chemical parameters

The suitability of water for drinking purpose can be judged through the content of physico-chemical parameters present in water. Four different drinking water samples collected from different areas of the *'Malwa'* region were tested to check concentration of these parameters. The analysis was done for three physico-chemical parameters *viz.* TDS, conductivity and pH. For checking TDS, HM made TDS-3 meter was used. The pH of the water samples was checked by using Spectralab made Eco pH meter. Both of these instruments are available with Energy Laboratory, Thapar University, Patiala, India. Following guidelines were followed during analysis:

i. The testing beaker was thoroughly cleaned with distilled water to remove any impurities or chemical compounds initially present.
ii. Before analysis, shaking of the sample was done to make it homogenous.
iii. The calibration of the pH measuring instrument 'Eco-pH' was done before analysis by dipping the pH electrode into 7 pH buffer solution.
iv. The probe of both TDS meter and pH meter was placed at a proper location in the beaker.

Different physico-chemical parameters (TDS, conductivity and pH) observed in collected drinking water samples are reported in Table 5.1. An insight into permissible limits of different parameters for safe drinking water defined by WHO [WHO, 2011] and BIS (BIS limits IS10500:2012) [BIS, 2012] is given in Table 5.2.

Table 5.1: Physico-chemical parameters in collected drinking water samples

Serial No.	Parameter	Kotkapura	Faridkot	Sri Muktsar Sahib	Bathinda
01.	TDS	1880 ppm	810 ppm	1200 ppm	1700 ppm
02.	Conductivity	3.76 µs/cm	1.62 µs/cm	2.4 µs/cm	3.4 µs/cm
03.	pH	7.95	7.10	7.69	7.48

Table 5.2: Permissible limits of different physico-chemical parameters [WHO, 2011; BIS, 2012]

Serial No.	Parameter	Permissible limit	
		WHO	BIS
01.	TDS	600 ppm	500 ppm
02.	Conductivity	*	*
03.	pH	*	6.5 – 8.5

* Standard not established

It was noted that the concentration of TDS varies from 810 ppm to 1880 ppm in the collected water samples. The highest amount of TDS was observed in sample collected from Kotkapura (District: Faridkot) with concentration more than three times the defined permissible limit by BIS. Additionally, no collected drinking water sample was within TDS limits defined by both WHO and BIS. The range of conductivity for the collected water samples was 1.62 µs/cm – 3.76 µs/cm. The pH of the collected samples varied from 7.10 to 7.95 which was well within the limit defined by BIS. The samples which are above the safe limits defined by WHO and BIS are shown in Table 5.3.

Table 5.3: Samples within permissible limits of physico-chemical parameters

Serial No.	Parameter	Samples within permissible limits							
		Kotkapura		Faridkot		Sri Muktsar Sahib		Bathinda	
		WHO	BIS	WHO	BIS	WHO	BIS	WHO	BIS
01.	TDS	×	×	×	×	×	×	×	×
02.	Conductivity	-	-	-	-	-	-	-	-
03.	pH	-	√	-	√	-	√	-	√

× No
√ Yes

5.1.2. Content of heavy metals

The presence of heavy metals in drinking water beyond prescribed limits has many harmful effects on human health. Their presence can cause cancer, diarrhea, genetic disorders obstruct mental development and damage blood vessels [W.1]. As per studies conducted by Bajwa et al. [2015] and Sekhon and Singh [2013], the content of heavy metals and uranium is quite high in the *'Malwa'* belt of Punjab, India. So, the present study focuses on the heavy metal analysis too. For heavy metal analysis, Agilent made 4100 – MP-AES system available in the Sophisticated Analytical Instruments (SAI) Laboratories, Thapar University, Patiala, India was used. The collected drinking water samples were tested for the presence of five different heavy metals *viz.* Zn, Pb, Fe, Co and Cr. All these elements are having adverse effects on humans if present in large quantities. The samples were kept in the refrigerator in polyethylene bottles before transferring to the laboratory for analysis. To minimize any external metal contamination, all laboratory processing's were performed under clean working conditions. Furthermore, before analysis, the samples were thoroughly shaken for homogeneity.

The concentration of different heavy metals observed in the collected drinking water samples is given in Table 5.4 and maximum permissible limits of heavy metals in drinking water defined by WHO [WHO 2011] and BIS [BIS, 2012] are given in Table 5.5. It was noted that the concentration of many heavy metals was above the safe limits prescribed by WHO. The level of Zn in the water samples collected from Sri Muktsar Sahib and Bathinda was found to be multi times the prescribed limit defined by WHO. In addition to this, high Pb content was observed in the water samples of Kotkapura, Sri Muktsar Sahib and Bathinda. Similarly, the concentration of Fe was noticed to be higher than the BIS permissible limits in Sri Muktsar Sahib and Bathinda

water samples. The samples having heavy metals above the safe limits defined by WHO and BIS can be seen in Table 5.6.

Table 5.4: Concentration of different heavy metals in collected drinking water samples

Serial No.	Element	Concentration observed			
		Kotkapura	Faridkot	Sri Muktsar Sahib	Bathinda
01.	Zn	< 50 µg/l	< 50 µg/l	8270 µg/l	600 µg/l
02.	Pb	230 µg/l	< 50 µg/l	160 µg/l	260 µg/l
03.	Fe	290 µg/l	250 µg/l	1110 µg/l	500 µg/l
04	Co	< 100 µg/l	< 100 µg/l	< 100 µg/l	< 100 µg/l
05.	Cr	< 50 µg/l	< 50 µg/l	< 50 µg/l	< 50 µg/l

Table 5.5: Permissible limits of different heavy metals
[WHO, 2011; BIS 2012]

Serial No.	Element	Permissible limits	
		WHO	BIS
01.	Zn	10 µg/l	5000 µg/l
02.	Pb	10 µg/l	10 µg/l
03.	Fe	*	300 µg/l
04	Co	*	*
05.	Cr	50 µg/l	50 µg/l

* Standard not established

Table 5.6: Samples within permissible limit of heavy metals

Serial No.	Element	Samples within permissible limits							
		Kotkapura		Faridkot		Sri Muktsar Sahib		Bathinda	
		WHO	BIS	WHO	BIS	WHO	BIS	WHO	BIS
01.	Zn	#	√	#	√	×	×	×	√
02.	Pb	×	×	#	#	×	×	×	×
03.	Fe	-	√	-	√	-	×	-	×
04.	Co	-	-	-	-	-	-	-	-
05.	Cr	√	√	√	√	√	√	√	√

× No
√ Yes
cannot be defined

The reasons are many to support the presence of heavy metals and uranium in high concentrations in the drinking water samples of Punjab, India. Different reasons given by various researchers in the past are summarized below in Table 5.7.

Table 5.7: Reasons for the poor quality of water given in various past studies

Serial No.	Researcher(s) and year of study	Reasons
01.	Bajwa et al. [2015]	• Anthropogenic activities • Use of fertilizers/pesticides on large extent • Industrialization and urbanization
02.	Tripathi et al. [2013]	• Chemical waste of industries • Excessive use of phosphate fertilizers for agriculture • Bad human activities and natural geology of the region
03.	Sekhon and Singh [2013]	• Domestic refuse and poor solid waste management • Anthropogenic and natural processes • High usage of mineral phosphate fertilizers
04.	Singh [2008]	• Industrial effluents in flowing canal water • Use of fertilizers/pesticides to boost agricultural production • Fly ash from thermal power plants
05.	Mehra et al. [2007]	• High radioactivity of granite rich rocks of Tusham hills, Bhiwani area, Haryana, India

5.2. Distillation rates at varying loads and compression ratios

It was found that the drinking water sample collected from Sri Muktsar Sahib, Punjab contains large content of both physico-chemical parameters and heavy metals. So, distillation was performed using this water sample. The supplied fresh ground water was preheated in the condenser and its temperature reached a value of approximately 50 ^{o}C. This preheated water was stored in the hot ground water storage tank having a total capacity of 27 liters. Before experimentation, the storage tank was sufficiently cleaned to remove any contaminants present. The ground water at 50 ^{o}C was than passed to the evaporator through ball control valve which ensured a controlled supply of 3 LPH of preheated ground water to the evaporating unit.

In the evaporator, the waste heat of exhaust flue gas was transferred to the incoming ground water forming steam, which was passed to the condenser using stainless steel wire braided pipe. In the condenser, the steam was condensed and resulted in the formation of distilled water. Distilled water was collected in the distilled water storage tank. The tank was cleaned thoroughly before experimentation. The experiments for the distillation of ground water were performed at five loading conditions *i.e.* 2 kg, 4kg, 6 kg, 8 kg and 10 kg, and four different compression ratios *viz.* 12:1, 14:1, 16:1 and 18:1. The volume of distilled water produced per

hour was measured with the help of height of the collected water in the distilled water storage tank.

The test was run nearly for 90 minutes at each loading condition. So, at a particular compression ratio and loading condition, each test takes a total time of 90 minutes. Initially, the distillation rate was quite low but it has increased 30 minutes after the start of the test. It may have become possible due to more heat availability and stabilization of exhaust flue gas temperature after this time period. Figure 5.1 shows the variation in collection rate of distilled water with load at a compression ratio of 12:1.

The effect of engine loading on temperature of the exhaust flue gas and actual extractable heat from the exhaust flue gas was seen in Fig. 4.2 and Fig. 4.4 respectively. As, the amount of heat that can be used for evaporation of ground water increases with load, therefore, an increase in distillation rate was also observed with increased loading.

Figure 5.2, Fig. 5.3 and Fig. 5.4 shows the variation in distilled water collection rate with load at different compression ratios *i.e.* 14:1, 16:1 and 18:1 respectively. It can be seen that the amount of distilled water produced reduces with increase in the compression ratio. This has become possible due to lower exhaust gas temperature and heat availability for the evaporation of ground water at higher compression ratios.

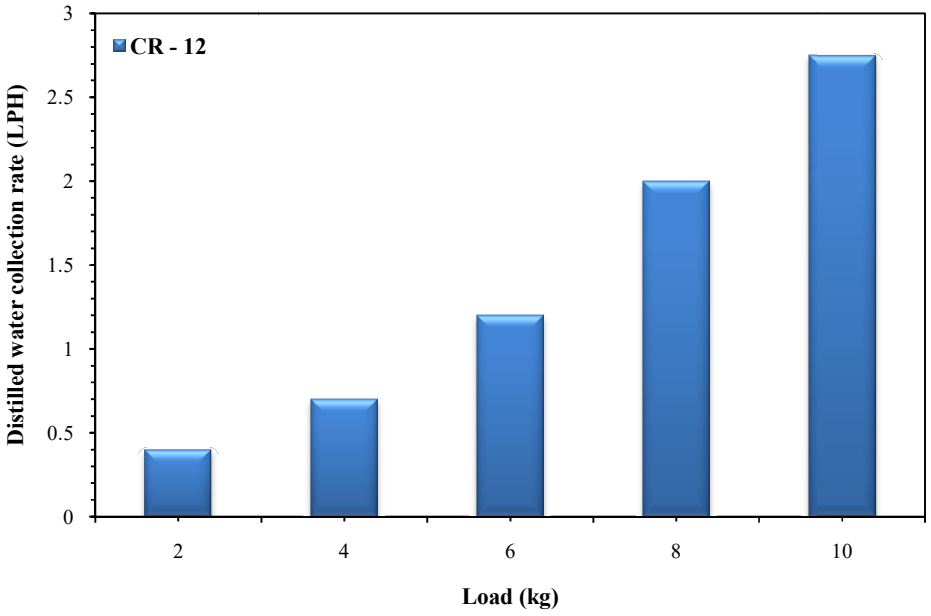

Figure 5.1: Variation of distilled water collection rate with load
(At CR – 12:1)

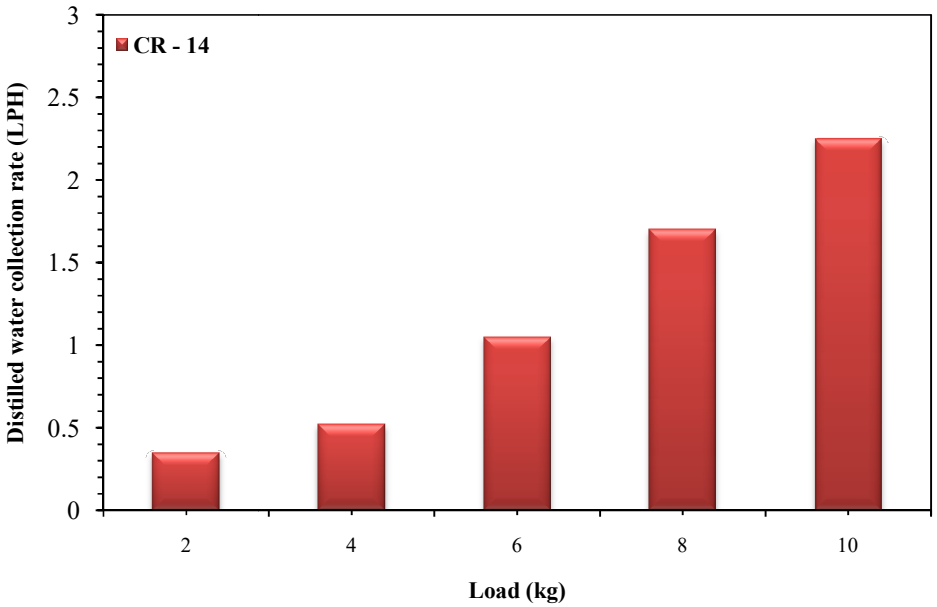

Figure 5.2: Variation of distilled water collection rate with load
(At CR – 14:1)

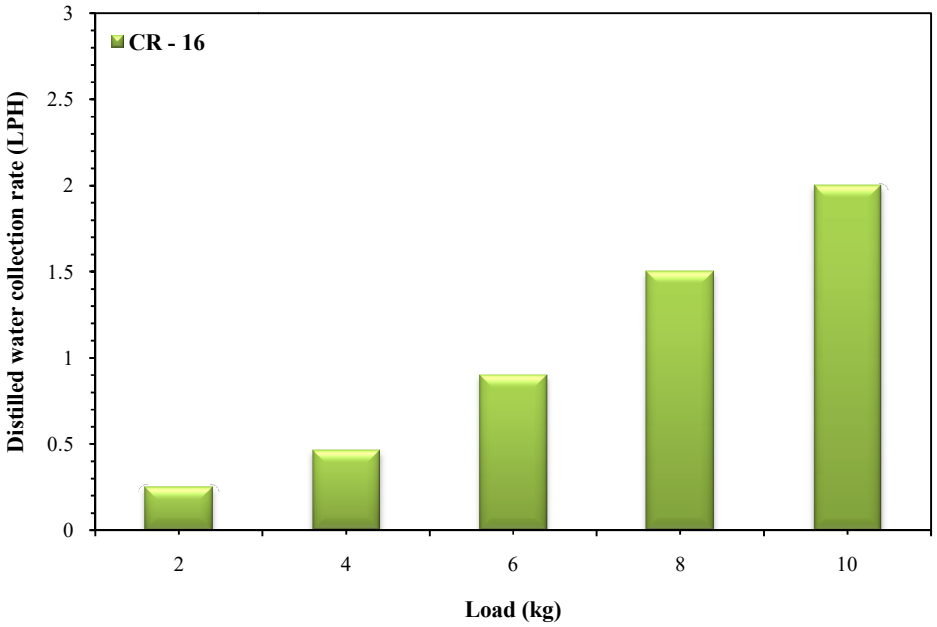

Figure 5.3: Variation of distilled water collection rate with load
(At CR – 16:1)

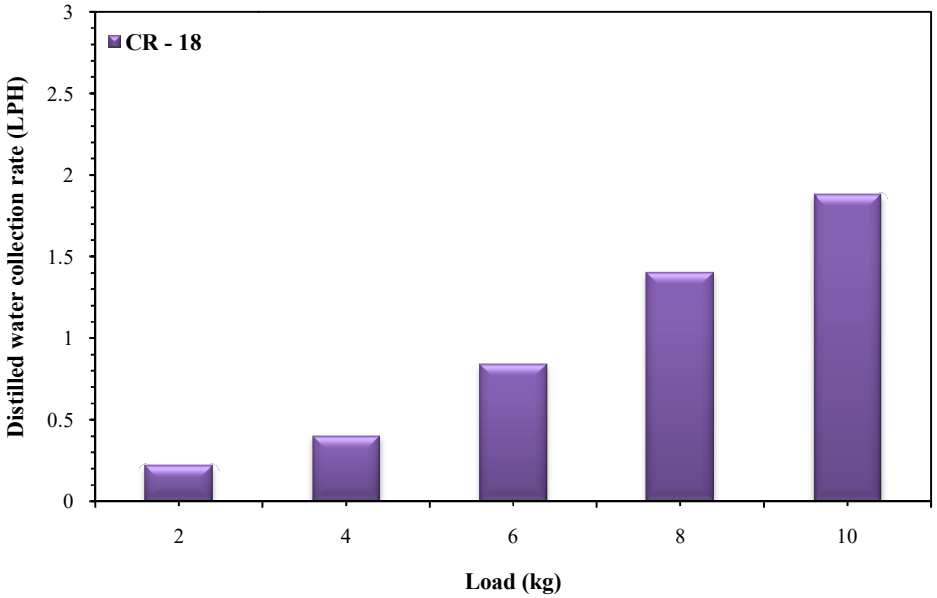

Figure 5.4: Variation of distilled water collection rate with load
(At CR – 18:1)

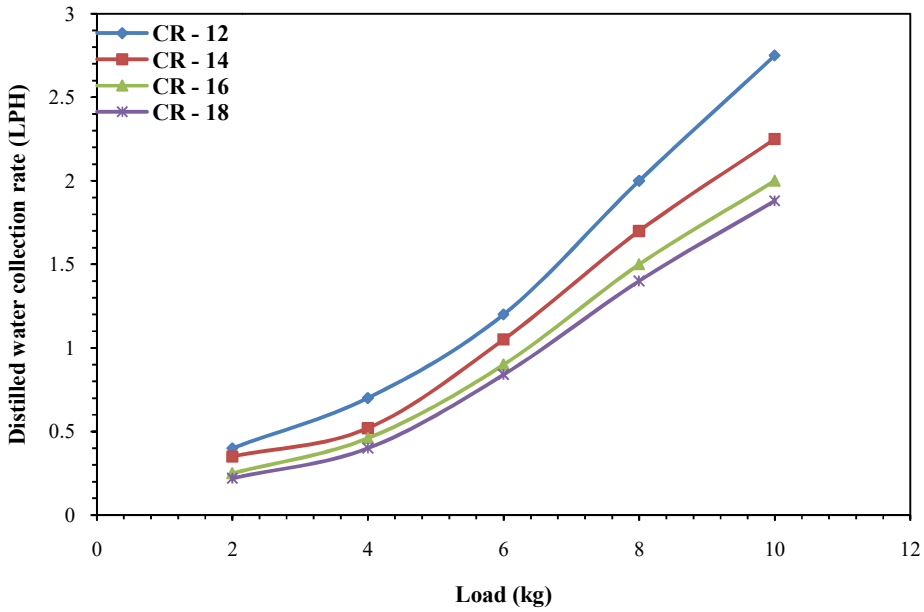

Figure 5.5: Variation of distilled water collection rate with load
(At varying compression ratios)

Figure 5.5 illustrates distilled water collection rates at varying loads and compression ratios. The maximum collection rate per hour was found to be 2.75 liters which was obtained at

12:1 compression ratio and 10 kg load, and the minimum collection rate per hour noted was 0.22 liters per hour obtained at 18:1 compression ratio and 2 kg load. Finally, the obtained distilled water was collected in a polyethylene bottle and stored at a low temperature in a dark room (preferably refrigerator) before transferring it to the laboratory for further analysis.

5.3. Tests after distillation

5.3.1. Physico-chemical parameters

After performing distillation, the collected distilled water was tested again for physico-chemical parameters (TDS, conductivity and pH). All the guidelines discussed above were again followed. The analysis was done using TDS-3 and Eco pH meters. Noted amount of different physico-chemical parameters in distilled water is given in Table 5.8. The content of TDS was found to be 39 ppm after distillation which was 1200 ppm before distillation. The TDS level in distilled water was well below the limit defined by WHO and BIS. The conductivity was changed from 2.4 µs/cm before distillation to 0.078 µs/cm after distillation. However, as distillation makes the water mild acidic, the value of pH did not fall in the permissible range defined by BIS. So, neutralizing materials like calcium carbonate (for pH > 6) or magnesium oxide (for pH < 6) are required to be added to increase the pH of distilled water before it is used for drinking purpose.

Table 5.8: Physico-chemical parameters in obtained distilled water

Serial No.	Parameter	Distilled water	Samples within permissible limits	
			WHO	BIS
01.	TDS	39 ppm	√	√
02.	Conductivity	0.078 µs/cm	-	-
03.	pH	5.62	-	×

× No
√ Yes

5.3.2. Content of heavy metals

The amount of different heavy metals present in obtained distilled water is shown in Table 5.9. The analysis for the presence of heavy metals was done using Agilent made 4100 – MP-AES system. The Zn content in the water sample was 150 µg/l after distillation and 8270 µg/l before distillation. So, its concentration was well below the limit defined by BIS. Also, the

concentration of Pb and Fe has decreased from 160 µg/l and 1110 µg/l to <50 µg/l and <100 µg/l respectively. Moreover, the amount of Co and Cr present was below the limits defined by WHO and BIS.

Table 5.9: Concentration of heavy metals present in obtained distilled water

Serial No.	Element	Amount present	Samples within permissible limits	
		Distilled water	WHO	BIS
01.	Zn	150 µg/l	×	√
02.	Pb	< 50 µg/l	#	#
03.	Fe	< 100 µg/l	-	√
04.	Co	< 100 µg/l	-	-
05.	Cr	< 50 µg/l	√	√

× No
√ Yes
cannot be defined

Although the concentration of physico-chemical parameters and heavy metals in the obtained distilled water was well below the limits defined by WHO and BIS yet this water can never be used for drinking purpose. It has been found that distillation also removes the essential minerals like Mg, Ca, K, Na and F- required for the growth of human body. So, before distilled water is used for drinking purpose, mineralization is needed to be done. In mineralization, the minerals required for the overall growth of human body are added to the water [W.21]. After increasing pH and mineralization, the obtained distilled water is fit for drinking purpose.

5.4. Comparison between distilled and RO water

5.4.1. For physico-chemical parameters

A comparison of purity level with respect to physico-chemical parameters like TDS, conductivity and pH in distilled water and RO water is given in Table 5.10. It has been found that the TDS level of both water samples was below the permissible limit defined by WHO and BIS. The conductivity of distilled water was lower than RO water. Additionally, it was noted that, pH value of both water samples was below the BIS permissible limit. So, in both water samples pH has to be increased to make them fit for drinking purpose.

Table 5.10: Comparison for physico-chemical parameters

Serial No.	Parameter	Amount Present		Samples within permissible limits			
		Distillation	Reverse Osmosis (RO)	Distillation		RO	
				WHO	BIS	WHO	BIS
01.	TDS	39 ppm	60 ppm	√	√	√	√
02.	Conductivity	0.078 µs/cm	0.12 µs/cm	-	-	-	-
03.	pH	5.62	6.39	×	×	×	×

× No
√ Yes

5.4.2. For heavy metals

The content of different heavy metals present in the obtained distilled water and RO water is given in Table 5.11. The concentration of Zn was found to be more in RO water as compared to distilled water. However, content of other heavy elements was same in both distilled water and RO water. So, both water samples were having approximately equal purity level as far as presence of heavy metals is concerned. In addition to this, there are two disadvantages associated with RO unit, firstly, large amount of water goes waste during purification and secondly, the membrane of the water purifier is needed to be changed periodically resulting in economic losses.

Table 5.11: Comparison for heavy metals

Serial No.	Element	Amount Present		Samples within permissible limits			
		Distillation	Reverse Osmosis (RO)	Distillation		RO	
				WHO	BIS	WHO	BIS
01.	Zn	150 µg/l	70 µg/l	×	√	×	√
02.	Pb	< 50 µg/l	< 50 µg/l	#	#	#	#
03.	Fe	< 100 µg/l	< 100 µg/l	-	√	-	√
04.	Co	< 100 µg/l	< 100 µg/l	-	-	-	-
05.	Cr	< 50 µg/l	< 50 µg/l	√	√	√	√

× No
√ Yes
cannot be defined

5.5. Total cost and payback period

The total cost of a particular system basically includes fabrication cost and operation and maintenance (O & M) cost. The fabrication cost of the various components, O & M cost (due to scaling, fouling and system damage) and approximate total cost of the proposed water purification unit are given in the Table 5.12 below. The fabrication cost of the unit was found to be ₹ 12000. The O & M cost per year was considered to be 10% of the total fabrication cost i.e. ₹ 1200. Therefore, the total cost of the proposed water purification unit will be ₹ 13200.

The total cost of the water purification unit changes with the power rating of the engine, required rate of distillation and design of heat exchangers. The cost analysis presented here is for an engine having rated power 3.5 kW and a maximum distillation rate of 2.75 liters/hour.

Table 5.12: Approximate total cost of the system

Serial No.	Name of the component	Fabrication cost
01.	Evaporator	₹ 3500
02.	Condenser	₹ 2500
03.	Control valve	₹ 300
04.	Pipes	₹ 1500
05.	Ground water storage tank	₹ 1000
06.	Distilled water storage tank	₹ 500
07.	Gaskets	₹ 200
08.	Drilling/welding	₹ 500
09.	Insulation & cladding	₹ 1000
10.	Miscellaneous components	₹ 1000
Total fabrication cost = ₹ 12000		
Operation and maintenance cost/year = ₹ 1200		
Approximate total cost = ₹ 13200		

Table 5.13: Payback period of the unit at different working conditions
(At CR – 12:1 and 10 kg load)

Serial No.	Running time of the engine (per day)	Distilled water production rate (per hour)	Total days (per year)	Distilled water production rate (per year)	Payback period
01.	6 hours	2.75 liters	300	4950 liters	2.7 years
02.	8 hours	2.75 liters	300	6600 liters	2 years
03.	10 hours	2.75 liters	300	8250 liters	1.6 years

Using the RO technique, the cost of producing fresh water per liter is ₹ 1 [Maheswari et al., 2015]. However, there will be no production cost with this system as it works purely on the basis of waste heat recovery. So, this system will result into economic benefits too. Considering the maximum production rate (at 12:1 compression ratio and 10 kg load), the payback periods of the proposed system under different working conditions are given in Table 5.13. The payback period vary between 1.6 years to 2.7 years depending upon the running time of the engine.

Table 5.14: Payback period of the unit at different working conditions
(At CR – 18:1 and 10 kg load)

Serial No.	Running time of the engine (per day)	Distilled water production rate (per hour)	Total days (per year)	Distilled water production rate (per year)	Payback period
01.	6 hours	1.88 liters	300	3384 liters	4 years
02.	8 hours	1.88 liters	300	4512 liters	3 years
03.	10 hours	1.88 liters	300	8250 liters	2.4 years

Diesel engines are generally run on high compression ratios. Therefore, considering the engine to be running on 18:1 compression ratio and 10 kg load, the payback periods for different running hours of the engine are given in Table 5.14. It has been found that if the engine runs for 8 hours per day, the payback period of the proposed water purification unit will be 3 years.

Chapter 6

Conclusions and future prospects

The aim of this thesis is to design a water purification unit working on the basis of exhaust waste heat recovery of variable compression ratio diesel engine available in the IC engines laboratory of Thapar University, Patiala, India. This chapter will discuss the conclusions and future prospects of this work.

6.1. Conclusions

The conclusions drawn from this work are summarized below:

i. Maximum extractable heat from the exhaust flue gas of the diesel engine that can be used for the distillation purpose was 1.68 kW at 12:1 compression ratio and 10 kg load. Based upon this maximum extractable heat, the evaporator and condenser of the water purification unit were designed and fabricated.

ii. The collected drinking water samples from four different areas of Punjab were tested for physico-chemical perimeters (TDS, conductivity and pH) and heavy metals (Zn, Pb, Fe, Co and Cr). Although the pH of the collected samples was well within the permissible limit defined by both WHO and BIS yet the amount of TDS found in all samples was quite high. The highest amount was observed in sample collected from Kotkapura (District: Faridkot) which was having concentration more than three times the defined permissible limit by WHO and BIS. Moreover, the level of zinc, lead and iron was found to be higher than their respective permissible limits defined by WHO in samples collected from Kotkapura, Sri Muktsar Sahib and Bathinda.

iii. The distilled water collection rate was found to be directly proportional to the amount of recoverable heat from the diesel engine. The maximum collection rate per hour was 2.75 liters which was obtained at 12:1 compression ratio and 10 kg load and the minimum collection rate per hour was 0.22 liters obtained at 18:1 compression ratio and 2 kg load.

iv. The level of physico-chemical parameters and heavy metals in the resulting distilled water was found to be well below the permissible limits defined by both WHO and BIS. But, the pH was noted to be lower than the defined limit. Moreover, as the distillation removes the health beneficial minerals too, therefore, neutralization and mineralization are needed to be done before this water can be made fit for drinking purpose.

v. The purity level of both distilled and RO water was noted to be approximately same with respect to the prescribed limits of both WHO and BIS. The payback period of the proposed water purification unit for the normal working of 8 hours per day, at maximum collection rate was found to be 2 years. However, if the diesel engine is run at a higher compression ratio of 18:1 and at 10 kg load, for 8 hours per day, than it will be 3 years.

The designed water purification unit can be integrated with stationary IC engines to produce distilled water. Additionally, ship engines can also be equipped with bigger desalination units working on the same principle. Therefore, with further advancements, these water purification units can address water scarcity issues of Punjab and other parts of the World, impacting large population in the long run.

6.2. Future prospects

The future prospects of this work will include the following:

i. The distilled water collection rate can be increased by enhancing the heat transfer. For this, in the evaporator, baffle plates can be inserted with proper spacing between them. Also, the gap between the shell and baffle plates can be blocked by installing sealers. The installation of sealers on the shell side of the evaporating unit will reduce the short circuit flow resulting in the surge of heat transfer rate.

ii. Solar energy can be utilized to increase the temperature of the ground water before it is stored in the hot water storage tank. This increase in temperature of the ground water will increase the production rate of distilled water.

iii. The design of the heat exchangers can be optimized by using computational fluid dynamics (CFD). This optimization will help in increasing the distilled water collection rate and decreasing the overall cost of the system.

iv. Other techniques like flash evaporation, multi-stage flash distillation (MSF) and multiple effect distillation (MED) can also be used for the purification of water. Using these techniques, the distilled water collection rate will increase.

v. More appropriate materials can be used for the fabrication of heat exchangers. In addition to this, control as well as prevention of scaling and corrosion will decrease the operation and maintenance cost of the water purification unit.

References

Bari, S.; Hossain, S.F. (2013) Waste heat recovery from a diesel engine using shell and tube heat exchanger. *Applied Thermal Engineering*, 61: 355–363.

Bajwa, B.S.; Kumar, S.; Singh, S.; Sahoo, S.K.; Tripathi, R.M. (2015) Uranium and other heavy toxic elements in the drinking water samples of SW-Punjab, India. *Journal of Radiation Research and Applied Sciences*, 30: 1–9.

BIS. (2012) Indian Standard DRINKING WATER – SPECIFICATION (Second Revision). Bureau of Indian Standards, New Delhi (www.cgwb.gov.in/Documents/WQ-standards .pdf).

Cardona, E.; Piacentino, A.; Marchese, F. (2007) Performance evaluation of CHP hybrid seawater desalination plants. *Desalination,* 205: 1–14.

Çengel, Y.A. (2007) Heat and Mass Transfer: A Practical Approach. Tata McGraw Hill Publishing Company Limited, New Delhi.

Duparchy, A.; Leduc, P.; Bourhis, G.; Ternal, C. (2009) Heat recovery for next generation of hybrid vehicles: simulation and design of a Rankine cycle system. *World Electric Vehicle Journal,* 3: 440–456.

Faizal, M.; Ahmed, M.R. (2012) Experimental studies on a corrugated plate heat exchanger for small temperature difference applications. *Experimental Thermal and Fluid Science,* 36: 242–248.

Hasanuzzaman, M.; Saidur, R.; Rahim, N.A. (2011) Energy, exergy and economic analysis of an annealing furnace. *International Journal of Physical Sciences,* 6(6): 1257–1266.

He, M.; Zhang, X.; Zeng, K.; Gao, K. (2011) A combined thermodynamic cycle used for waste heat recovery of internal combustion engine. *Energy,* 36: 6821–6829.

Hountalas, D.T.; Mavropoulos, G.C.; Katsanos, C.; Knecht, W. (2012) Improvement of bottoming cycle efficiency and heat rejection for HD truck applications by utilization of EGR and CAC heat. *Energy Conversion and Management,* 53(1): 19–32.

Ibaraki, S.; Endo, T.; Kojima, Y.; Takahashi, K.; Baba, T.; Kawajiri, S. (2007) Study of efficiency on-board waste heat recovery system using Rankine cycle. *Review of Automotive Engineering,* 28: 307–313.

Jadhao, J.S.; Thombare, D.G. (2013) Review on Exhaust Gas Heat Recovery for I.C. Engine. *International Journal of Engineering and Innovative Technology,* 2(12): 93–100.

Jamshidi, N.; Farhadi, M.; Ganji, D.D; Sedighi, K. (2013) Experimental analysis of heat transfer enhancement in shell and helical tube heat exchangers. *Applied Thermal Engineering,* 51: 644–652.

Jia, S.; Peng, H.; Liu, S.; Zhang, X. (2009) Review of transportation and energy consumption related research. *Journal of Transportation Systems Engineering and Information Technology,* 9(3): 6–16.

Kakac, S. (1991) Boilers, Evaporators, and Condensers. John Wiley & Sons Inc, Toronto.

Kalogirou, S.A. (2001) Design of a new spray-type seawater evaporator. *Desalination,* 139: 345–352.

Kara, Y.A.; Güraras, Ö. (2004) A computer program for designing of shell-and-tube heat exchangers. *Applied Thermal Engineering,* 24: 1797–1805.

Karagiannis, I.C.; Soldatos, P.G. (2008) Water desalination cost literature: review and assessment. *Desalination,* 223: 448–456.

Khawaji, A.D.; Kutubkhanah, I.K.; Wie, J.M. (2008) Advances in seawater desalination technologies. Desalination, 221: 47–69.

Kundu, B. (2015) Beneficial design of unbaffled shell-and-tube heat exchangers for attachment of longitudinal fins with trapezoidal profile. *Case Studies in Thermal Engineering,* 5: 104–112.

Lattemann, S.; Hopner, T. (2008) Environmental impact and impact assessment of seawater desalination. *Desalination,* 220: 1–15.

Lee, D.H.; Lee, J.D.; Park, J.S. (2010) Effects of secondary combustion on efficiencies and emission reduction in the diesel engine exhaust heat recovery system, *Applied Energy,* 87: 1716–1721.

Maheswari, K.S.; Murugavel, K.K.; Esakkimuthu, G. (2015) Thermal desalination using diesel engine exhaust waste heat – An experimental analysis. *Desalination,* 358: 94–100.

Markowski, M.; Trafczynski, M.; Urbaniec, K. (2013) Identification of the influence of fouling on the heat recovery in a network of shell and tube heat exchangers. *Applied Energy,* 102: 755–764.

Medrano, M.; Yilmaz, M.O.; Nogues, M.; Martorell, I.; Roca, J.; Cabeza, L.F. (2009) Experimental evaluation of commercial heat exchangers for use as PCM thermal storage systems. *Applied Energy,* 86: 2047–2055.

Mehra, R.; Singh, S.; Singh, S. (2007) Uranium studies in water samples belonging to Malwa region of Punjab, using track etching technique. *Radiation Measurements,* 42: 441–445.

Moore, B.A.; Martinson, E.; Raviv, D. (2008) Waste to water: a low energy water distillation method. *Desalination,* 220: 502–505.

Pandiyarajan, V.; Pandiyan, M.C.; Malan, E.; Velraj, R.; Seeniraj, R.V. (2011) Experimental investigation on heat recovery from diesel engine exhaust using finned shell and tube heat exchanger and thermal storage system. *Applied Energy,* 88: 77–87.

Pickerill, K. (2010) Automotive engine performance. Cengage Learning, Massachusetts.

Pogiatzis, T.; Ishiyama, E.M.; Paterson, W.R.; Vassiliadis, V.V.; Wilson, D.I. (2012) Identifying optimal cleaning cycles for heat exchangers subject to fouling and ageing. *Applied Energy,* 89: 60–66.

Rahman, H.; Hawlader, M.N.A.; Malek, A. (2003) An experiment with a single-effect submerged vertical tube evaporator in multi-effect desalination. *Desalination,* 156: 91–100.

Saidur, R.; Rezaei, M.; Muzammil, W.K.; Hassan, M.H.; Paria, S.; Hasanuzzaman, M. (2012) Tehnologies to recover exhaust heat from internal combustion engines. *Renewable and Sustainable Energy Reviews,* 16: 5649–5659.

Salimpour, M.R. (2009) Heat transfer coefficients of shell and coiled tube heat exchangers. *Experimental Thermal and Fluid Science,* 33: 203–207.

Sekhon, G.S.; Singh, B. (2013) Estimation of Heavy Metals in the Groundwater of Patiala District of Punjab, India. *Earth Resources*, 1(1): 1–4.

Singh, B.P. (2008) Cancer Deaths in Agricultural Heartland A study in Malwa Region of Indian Punjab, M.Sc Thesis, International Institute for Geo-Information Science and Earth observations, Enschede, The Netherlands (https://www.itc.nl/library/papers_2008/msc/gem/bajinderpdf.pdf).

Sommariva, C. (2008) Utilisation of power plant waste heat streams to enhance efficiency in thermal desalination. *Desalination,* 222: 592–595.

Tanaka, H.; Park, C.D. (2010) Distillation utilizing waste heat from a portable electric generator. *Desalination,* 258: 136–142.

Taymaz, I. (2006) An experimental study of energy balance in low heat rejection diesel engine. *Energy,* 31: 364–371.

Tripathi, R.M.; Sahoo, S.K.; Mohapatra, S.; Lenka, P.; Dubey, J.S.; Puranik, V.D. (2013) Study of uranium isotopic composition in groundwater and deviation from secular equilibrium condition. *Journal of Radioanalytical and Nuclear Chemistry,* 295: 1195–1200.

Vaja, I.; Gambarotta, A. (2010) Internal combustion engine (ICE) bottoming with organic Rankine cycles (ORCs). *Energy,* 35(2): 1084–1093.

Wang E.H.;, Zhang, H.G.; Fan, B.Y.; Ouyang, M.G.; Zhao, Y.; Mu, Q.H. (2011) Study of working fluid selection of organic Rankine cycle (ORC) for engine waste heat recovery. *Energy,* 36: 3406–3418.

Wang, S.; Wen, J.; Li, Y. (2009) An experimental investigation of heat exchanger enhancement for a shell-and-tube heat exchanger. *Applied Thermal Engineering,* 29: 2433–2438.

Will, F. (2012) Fuel conservation and emission reduction through noval waste heat recovery for internal combustion engines. *Fuel,* 102: 247–255.

WHO. (2011) Guidelines for Drinking-water Quality. World Health Organization, Geneva (www .who.int/water_sanitation_health/publications/dwq-guideline s-4en/).

Yu, C.; Chau, K.T. (2009) Thermoelectric automotive waste heat energy recovery using maximum power point tracking. *Energy Conversion and Management,* 50: 1506–1512.

Yüksel, F.; Ceviz, M. (2003) Thermal balance of a four stroke SI engine operating on hydrogen as a supplement fuel. *Energy,* 28: 1069–1080.

Zhang, H.G.; Wang, E.H.; Fan, B.Y. (2013) Heat transfer analysis of a finned-tube evaporator for engine exhaust heat recovery. *Energy Conversion and Management,* 65: 438–447.

Web References

W.1 Adverse health effects of heavy metals in children, www.who.int/ceh/capacity/heavy_metals.pdf, (accessed on 06/04/2016).

W.2 Basic information, www.fchart.com/ees/heat_transfer_library/compact_hx/hs_100.html, (accessed on 19/07/2015).

W.3 Diesel exhaust gas, https://www.dieselnet.com/tech/diesel_exh.php, (accessed on 16/09/2015).

W.4 Distillation, https://en.wikipedia.org/wiki/Distillation, (accessed on 11/05/2015).

W.5 Distillation, www.ssc.education.edu.ac.uk/BSL/chemistry/distillation.html, (accessed on 21/05/2015).

W.6 Districts of Punjab, www.punjab.gov.in/districts, (accessed on 14/12/2015).

W.7 Districts map of Punjab, http://www.mapsofindia.com/maps/punjab/punjabdistrict.htm, (accessed on 21/12/2016).

W.8 Flue gases properties table, http://www.pipeflowcalculations.com/tables/flue-gas.php, (accessed on 18/09/2015).

W.9 Ion exchange, https://en.wikipedia.org/wiki/Ion_exchange, (accessed on 25/04/2015).

W.10 MAIN SOURCE OF DRINKING WATER & ITS AVAILABILITY 2001 & 2011, www.punjabcensus.gov.in/pdf/Drinking%20water.pdf, (accessed on 06/01/2016).

W.11 Plate Heat Exchanger & Services, www.indiamart.com, (accessed on 21/07/2015).

W.12 Reverse osmosis, https://en.wikipedia.org/wiki/Reverse_osmosis, (accessed on 28/04/2015).

W.13 Thermal Conductivity of some common Materials and Gases, http://www.engineeringtoolbox.com/thermalconductivityd_429.html, (accessed on 27/09/2015).

W.14 The Structure of Plate Heat Exchanger, http://www.ddqcw.com/bbs/thread-134843-1-1.html, (accessed on 27/07/2015).

W.15 Viscosity, https://en.wikipedia.org/wiki/Viscosity, (accessed on 21/09/2015).

W.16 Water, https://en.wikipedia.org/wiki/Water, (accessed on 08/04/2015).

W.17 Water purification, https://en.wikipedia.org/wiki/Water_purification, (accessed on 23/04/2015).

W.18 Water sampling and analysis, www.who.int/water_sanitation_health/dwq/2edvol3d .pdf, (accessed on 11/01/2016).

W.19 Water scarcity, https://en.wikipedia.org/wiki/Water_scarcity.pdf, (accessed on 14/04/2015).

W.20 Water – Thermal Properties, http://www.engineeringtoolbox.com/waterthermalpropertiesd_1 62.html, (accessed on 28/09/2015).

W.21 Which Minerals Should You Add to Distilled Water Before Drinking, http://www.livestrong.com/article/500898-what-minerals-should-you-add-to-distilled-water-before-drinking, (accessed on 11/03/2016).

APPENDIX: A1

Table A1.1: Combustion parameters of the VCRE

Specific gas constant (kJ/kgK)	Air density (kg/m^3)	Adiabatic index	Polytrophic index
1.00	1.17	1.41	1.26

Table A1.2: Performance parameters of the VCRE

Orifice diameter (m)	Orifice coefficient of discharge	Dynamometer arm length (m)	Fuel pipe diameter (m)	Ambient temperature (K)
0.02	0.60	0.185	0.0124	300

Table A1.3: Details of the fuel used in the VCRE

Type of fuel	Fuel density (kg/m^3)	Calorific value of fuel (kJ/kg)
Diesel	820	44630

Table A1.4: VCRE data at different loading conditions (At CR – 12:1)

Load (kg)	$\dot{m}_e$ (kg/s)	T_{ei} (K)	$Q_{max.}$ (kW)	Q_e (kW)
2	0.00786	466.92	1.31	0.58
4	0.00792	486.71	1.47	0.74
6	0.00797	515.49	1.71	0.97
8	0.00804	559.03	2.08	1.33
10	0.00810	600.77	2.43	1.68

Table A1.5: VCRE data at different loading conditions (At CR – 14:1)

Load (kg)	$\dot{m}_e$ (kg/s)	T_{ei} (K)	$Q_{max.}$ (kW)	Q_e (kW)
2	0.00791	440.75	1.11	0.53
4	0.00799	468.33	1.34	0.60
6	0.00805	501.33	1.62	0.87
8	0.00808	536.44	1.91	1.15
10	0.00818	589.54	2.37	1.60

Table A1.6: VCRE data at different loading conditions (At CR – 16:1)

Load (kg)	$\dot{m}_e$ (kg/s)	T_{ei} (K)	$Q_{max.}$ (kW)	Q_e (kW)
2	0.00795	437.06	1.09	0.35
4	0.00805	465.55	1.32	0.58
6	0.00807	491.62	1.48	0.79

8	0.00813	524.96	1.74	1.07
10	0.00824	572.05	2.17	1.47

Table A1.7: VCRE data at different loading conditions (At CR – 18:1)

Load (kg)	$\dot{m}_e$ (kg/s)	T_{ei} (K)	$Q_{max.}$ (kW)	Q_e (kW)
2	0.00801	433.25	1.06	0.32
4	0.00811	460.95	1.27	0.55
6	0.00814	484.51	1.45	0.74
8	0.00822	514.94	1.70	1.01
10	0.00831	536.51	2.15	1.41

APPENDIX: A2

Table A2.1: Design values for evaporator

Parameter	Value	Unit
A_{he}	0.15	m^2
C_e	1.21	kJ/kgK
C_{gw}	4.18	kJ/kgK
d_{ei}	0.012	m
d_{esi}	0.140	m
d_{eo}	0.014	m
FR_{ei}	0.001761	m^2K/W
FR_{eo}	0.000176	m^2K/W
K_e	0.0466	W/mK
K’	370	W/mK
l_e	0.50	m
l_{es}	0.780	m
L_{gw}	2257	kJ/kg
$\dot{m}_e$	0.00810	kg/s
$\dot{m}_{gw}$	8.33×10^{-4}	kg/s
N_e	7	-
T_{bw}	373	K
T_{ei}	600.77	K
T_{eo}	393	K
ΔT_{gw}	70	K
μ_e	37.6×10^{-6}	Pa.s
ρ_e	0.405	kg/m^3

Table A2.2: Design values for condenser

Parameter	Value	Unit
A_{hc}	0.025	m^2
C_c	0.61	-
C_d	4.22	kJ/kgK
C_{gw}	4.18	kJ/kgK
d_{ci}	0.012	m
d_{co}	0.014	m
d_{csi}	0.096	m
FR_{ci}	0.000176	m^2K/W
FR_{co}	0.000088	m^2K/W
h_f	419.04	kJ/kg
h_{fg}	2257	kJ/kg
K_{gw}	0.58	W/mK
K’	370	W/mK

l_c	0.58	m
l_{cs}	0.380	m
L_{gw}	2257	kJ/kg
L_{st}	- 2257	kJ/kg
$\dot{m}_{dw}$	7.63×10^{-4}	kg/s
N_c	1	-
P	0.315	-
R	2.739	-
T_{dwi}	373	K
T_{dwo}	310	K
T_{gwi}	323	K
T_{gwo}	300	K
ΔT_{gw}	23	K
ΔT_{dw}	63	K
μ_c	547.1×10^{-6}	Pa.s
ρ_c	988	kg/m^3

APPENDIX: A3

Table A3.1: Distilled water collection rate data at varying load conditions (At CR – 12:1)

Load (kg)	Length of the distilled water storage tank (m)	Breath of the distilled water storage tank (m)	Height of the distilled water storage tank (m)	Distilled water collection rate (LPH)
2	0.15	0.15	0.020	0.40
4	0.15	0.15	0.031	0.70
6	0.15	0.15	0.053	1.20
8	0.15	0.15	0.088	2
10	0.15	0.15	0.122	2.75

Table A3.2: Distilled water collection rate data at varying load conditions (At CR – 14:1)

Load (kg)	Length of the distilled water storage tank (m)	Breath of the distilled water storage tank (m)	Height of the distilled water storage tank (m)	Distilled water collection rate (LPH)
2	0.15	0.15	0.015	0.35
4	0.15	0.15	0.023	0.52
6	0.15	0.15	0.046	1.05
8	0.15	0.15	0.075	1.70
10	0.15	0.15	0.100	2.25

Table A3.3: Distilled water collection rate data at varying load conditions (At CR – 16:1)

Load (kg)	Length of the distilled water storage tank (m)	Breath of the distilled water storage tank (m)	Height of the distilled water storage tank (m)	Distilled water collection rate (LPH)
2	0.15	0.15	0.011	0.25
4	0.15	0.15	0.020	0.46
6	0.15	0.15	0.040	0.90
8	0.15	0.15	0.066	1.50
10	0.15	0.15	0.089	2

Table A3.4: Distilled water collection rate data at varying load conditions (At CR – 18:1)

Load (kg)	Length of the distilled water storage tank (m)	Breath of the distilled water storage tank (m)	Height of the distilled water storage tank (m)	Distilled water collection rate (LPH)
2	0.15	0.15	0.0098	0.22
4	0.15	0.15	0.018	0.40

6	0.15	0.15	0.037	0.84
8	0.15	0.15	0.062	1.40
10	0.15	0.15	0.083	1.88